Carbohydrate Polymers 256 (2021) 117594

Contents lists available at ScienceDirect

Carbohydrate Polymers

journal homepage: www.elsevier.com/locate/carbpol

Suppression of obesity and inflammation by polysaccharide from sporoderm-broken spore of *Ganoderma lucidum* via gut microbiota regulation

Tingting Sang [1], Chengjie Guo [1], Dandan Guo, Jianjun Wu, Yujie Wang, Ying Wang, Jiajun Chen, Chaojie Chen, Kaikai Wu, Kun Na, Kang Li, Liu Fang, Cuiling Guo, Xingya Wang *

College of Pharmaceutical Science, Zhejiang Chinese Medical University, Hangzhou, China

ARTICLE INFO

Keywords:
Obesity
Gut microbiota
Endotoxemia
Sporoderm-broken spores
Ganoderma lucidum polysaccharide

ABSTRACT

Ganoderma lucidum has been shown to have anti-obesity effects. However, polysaccharide extracted from the sporoderm-broken spores of *Ganoderma lucidum* (BSGLP) against obesity and its underlying mechanisms have never been reported. In the current study, we showed that BSGLP inhibited high-fat diet (HFD)-induced obesity, hyperlipidemia, inflammation, and fat accumulation in C57BL/6 J mice. BSGLP improved HFD-induced gut microbiota dysbiosis, maintained intestinal barrier function, increased short-chain fatty acids production and GPR43 expression, ameliorated endotoxemia, manifested by reduced serum lipopolysaccharide level, and increased ileum expression of tight junction proteins and antimicrobial peptides. Fecal microbiota transplantation study confirmed that BSGLP-induced microbiota change is responsible, at least in part, for obesity inhibition. Besides, BSGLP notably alleviated HFD-induced upregulation of TLR4/Myd88/NF-κB signaling pathway in adipose tissue. Collectively, our study showed for the first time that BSGLP might be used as a prebiotic agent to inhibit obesity and hyperlipidemia through modulating inflammation, gut microbiota, and gut barrier function.

1. Introduction

The prevalence of obesity has dramatically increased over the past decades, which has become a huge threat to human health worldwide (Collaboration, N. C. D. R. F., 2017). Both genetic susceptibility and environmental factors such as diet and lifestyle could contribute to obesity. The main characteristics of obesity are excessive weight gain and fat accumulation, which can cause chronic low-grade inflammation, high blood glucose, hyperlipidemia, and insulin resistance. These symptoms are associated with a variety of metabolic diseases such as type 2 diabetes mellitus, cardiovascular disease, non-alcoholic fatty liver disease (NAFLD), and cancers (Heymsfield & Wadden, 2017).

Recently, numerous clinical and experimental studies have demonstrated that gut microbiota plays a key role in the development and progression of obesity by regulating host energy metabolism, substrate metabolism, and inflammatory responses (Sommer & Backhed, 2013;

Abbreviations: AUC, area under the curve; BSGLP, GLP extracted from sporoderm-broken spores of *G. lucidum*; ELISA, enzyme-linked immunosorbent assay; eWAT, epididymal white adipose tissue; FMT, fecal microbiota transplantation; *G. lucidum*, *Ganoderma lucidum*; GLP, *G. lucidum* polysaccharide; GC–MS, gas chromatography-mass spectrometry; GPR41, G-protein coupled receptor 41; GPR43, G-protein coupled receptor 43; HFD, high-fat diet; HDL, high-density lipoprotein; IL-1β, interleukin-1 beta; IL-6, interleukin-6; IPGTT, intraperitoneal glucose tolerance test; iWAT, inguinal white adipose tissue; LBP, lipopolysaccharide-binding protein; LDA, linear discriminant analysis; LDL, low-density lipoprotein; LEfSe, linear discriminant analysis effect size; LFD, low-fat diet; LPS, lipopolysaccharide; Lyz1, lysozyme 1; MCP-1, monocyte chemotactic peptide-1; Myd88, myeloid differentiation primary response protein 88; NEFA, non-esterified fatty acid; NMDS, non-metric multidimensional scaling; OTU, operational taxonomic unit; PCA, principal component analysis; qRT-PCR, quantitative real-time PCR; Reg3γ, regenerating islet-derived protein 3-gamma; SCFAs, short-chain fatty acids; TC, total cholesterol ; TG, triglycerides; TLR4, toll-like receptor 4; TNF-α, tumor necrosis factor alpha; ZO-1, zonula occludens protein 1.

* Corresponding author at: College of Pharmaceutical Science, Zhejiang Chinese Medical University, 548 Binwen Road, Hangzhou, Zhejiang, 310053, China.
E-mail address: xywang@zcmu.edu.cn (X. Wang).

[1] These authors contributed equally to the study.

https://doi.org/10.1016/j.carbpol.2020.117594
Received 30 June 2020; Received in revised form 27 December 2020; Accepted 28 December 2020
Available online 4 January 2021

Turnbaugh et al., 2006; Ussar et al., 2015). Human studies have shown that the gut microbiota composition is significantly different between obese and non-obese individuals, with obese population have reduced diversity of microbiota (Sommer & Backhed, 2013; Sonnenburg & Backhed, 2016; Turnbaugh et al., 2009). Disruption of gut microbiota or dysbiosis can increase lipopolysaccharide (LPS) produced by gram-negative bacterial, which lead to impaired gut barrier function and cause endotoxemia (Fujisaka et al., 2018; Stevens et al., 2018; Zhao, 2013). LPS can enter the mesenteric vein, travel into circulation system, and act on target organs and tissues to cause inflammation and diseases (Fujisaka et al., 2018; Tilg, Zmora, Adolph, & Elinav, 2019).

Dietary intervention has been shown to have beneficial effects in ameliorating metabolic endotoxemia upon HFD (Anhe et al., 2018; Jiang et al., 2016). Dietary fibers and indigestible polysaccharides protect against HFD-induced obesity, intestinal dysbiosis, gut permeability, and endotoxemia, which is associated with increased diversity and functions of gut microbiota, such as the production of short-chain fatty acids (SCFAs) (Makki, Deehan, Walter, & Backhed, 2018). SCFAs are end products that are fermented from dietary fibers and indigestible polysaccharides by gut microbiota (Makki et al., 2018). Feeding the gut microbiota with dietary fiber, such as polysaccharides, could prevent the growth of mucus-degrading bacteria and increase the growth of SCFA-producing bacteria in the gut (Huo et al., 2020, Desai et al., 2016; Liu et al., 2020).

G. lucidum, a medicinal mushroom, has been used for promoting health, prolonging life, and preventing diseases in Asian countries for more than two thousand years (Bishop et al., 2015). *G. lucidum* polysaccharide (GLP), one of the main bioactive substances of *G. lucidum*, has been demonstrated to have many pharmacological functions such as immunomodulation, antioxidation, anti-inflammation, anti-tumors, anti-obesity, and antidiabetic effects (Bishop et al., 2015; Li, Zhang, & Zhong, 2011; Liang, Yuan, Li, Fu, & Shan, 2018). Recently, several studies have reported that GLP extracted from mycelium or fruiting body of *G. lucidum* could modulate gut microbiota composition, which may be associated with disease prevention, such as cancer and obesity (Chang et al., 2015; Chen et al., 2019; Khan et al., 2019; Xu et al., 2017). For example, Chang et al. found that GLP extracted from mycelium of *G. lucidum* could inhibit obesity and inflammation, increase insulin sensitivity, and improve lipid metabolic disorders via modulating gut microbiota and gut barrier function (Chang et al., 2015).

The sporoderm-broken spores of *G. lucidum* (BSGL) and their extracts also exhibited a wide range of biological activities. Many studies have characterized the chemical structure and composition of polysaccharides extracted from the spores, fruiting body, or mycelium of *G. lucidum*. Due to factors such as extraction methods and source of *G. lucidum* could all affect the results, it is difficult to compare the chemical properties of the polysaccharide extracted from different parts of *G. lucidum*. These studies in general suggest that GLP extracted from different parts of *G. lucidum* are different in molecular weight, monosaccharide composition, α/β configuration, glycosidic bond, and branching degrees (Chang et al., 2015; Fu, Shi, & Ding, 2019; Kim et al., 2014; Sun et al., 2014; Wang et al., 2017; Xu et al., 2019; Ye et al., 2008; Zhang et al., 2019). It has been reported that the differences in chemical properties of polysaccharides have certain influences on their pharmacological action (Hu et al., 2020; Li et al., 2020). Therefore, GLP extracted from different parts of *G. lucidum* may elicit different biological effects. At present, no study has reported the relationship between obesity and BSGLP. In addition, the molecular mechanisms underlying the anti-obesity effects of GLP remains largely unknown.

In the current study, we studied the effects of GLP extracted from BSGL (BSGLP) on body weight, fat accumulation, hyperglycemia, glucose tolerance, hyperlipidemia, and chronic inflammation in a mouse model of dietary-induced obesity. Changes in gut microbiota composition, HFD-induced endotoxemia, gut barrier function, SCFAs production, and underlying molecular mechanisms were also examined.

2. Materials and methods

2.1. Materials

Low-fat diet (LFD) consists of 10 % calories from fat (D12450 J), and HFD consists of 60 % calories from fat (D12492) were purchased from Research Diet (New Brunswick, NJ, USA). The iScript cDNA synthesis kit and SYBR master mix were purchased from Bio-Rad (Hercules, CA, USA). The bicinchoninic acid (BCA) assay kit was from Pierce (Rockford, IL, USA). The Western Lightening™ Plus-ECL Enhanced chemiluminescence Substrate assay kit was obtained from Perkin-Elmer (Waltham, MA, USA). Zonula occludens protein 1 (ZO-1) antibody (OM161091) was purchased from Omnimabs (Alhambra, CA, USA). Occludin antibody (13409-1-AP) was from Proteintech (Rosemont, IL, USA). Lysozyme 1 (Lyz1) antibody (BA0092) was from Boster Biological Technology (Wuhan, Hubei, China). Toll-like receptor 4 (TLR4) antibody (ab13556), G-protein coupled receptor 43 (GPR43) antibody (ab131003), and Claudin-1 antibody (ab15098) were from Abcam (Cambridge, UK). Myeloid differentiation primary response protein 88 (Myd88) (4283S), NF-κB (8242 s), phosphorylated NF-κB (p-NF-κB) (3033 s), and HRP-conjugated secondary antibody were all purchased from Cell Signaling Technology (Beverly, MA, USA). The β-actin antibody (db10001) was from Diagbio (Hangzhou, Zhejiang, China). CD68 antibody (GB11067) was from Wuhan Servicebio (Wuhan, Hubei, China). The enzyme-linked immunosorbent assay (ELISA) kits for detecting interleukin-1 beta (IL-1β) (MM-0040M1), interleukin-6 (IL-6) (MM-0163M1), tumor necrosis factor alpha (TNF-α) (MM-0132M1), monocyte chemotactic peptide-1 (MCP-1) (MM-0082M1), LPS (MM-0634M1), Occludin (MM-0942M1), Claudin-1 (MM-0941M1), regenerating islet-derived protein 3-gamma (Reg3γ) (MM-1114M1) were purchased from Jiangsu Meimian Industrial Co. Ltd (Yancheng, Jiangsu, China). Reagents to detect serum total cholesterol (TC) (A111-1-1), triglycerides (TG) (A110-1-1), non-esterified fatty acid (NEFA) (A042-1-1), high-density lipoprotein (HDL) (A112-1-1), and low-density lipoprotein (LDL) (A113-1-1) were obtained from Nanjing Jiancheng Bioengineering Institute (Nanjing, Jiangsu, China). The antibiotics ampicillin, metronidazole, vancomycin, and neomycin were purchased from Beijing Solarbio Science & Technology Co., Ltd. (Beijing, China).

2.2. Polysaccharide preparation

The powder of sporoderm-broken spores of *G. lucidum* was obtained from Shandong Zhengxin bio (Taian, Shandong, China). BSGLP was extracted from sporoderm-broken spores of *G. lucidum* through water extraction and ethanol precipitation as previously described (Pan et al., 2019). Then, the crude polysaccharides were de-proteinized through Sevag method, followed by freeze-drying using H051 freeze dryer of LaboGene (Lynge, Denmark) to obtain purified BSGLP for subsequent experiments. The total carbohydrate content of BSGLP was 80.87 ± 2.00 % as determined by the phenol-sulfuric acid colorimetric method. The Fourier transform infrared spectra of BSGLP displayed a typical polysaccharide's spectrum, which confirmed that the main chemical components of BSGLP were polysaccharides. High-performance gel permeation chromatography method with chromatographic column KS-804 and KS-802 in series was used to estimate the molecular weight distribution of BSGLP. The weight-average molecular weight of BSGLP was determined to be 26.0 kDa. BSGLP was composed of glucose, mannose, and galactose in a molar ratio of 87.4 : 4.81 : 8.14 as determined by gas chromatography as described previously (Wu et al., 2017). Based on the data of ^{13}C, DEPT135, and HSQC NMR spectrum, BSGLP was a β-D-glucan containing (1→3)-β-D-Glc*p*, (1→3,6)-β-D-Glc*p*, (1→6)-β-D-Glc*p*, and terminal-β-D-Glc*p* moieties.

2.3. Animal study

All the experimental procedures were performed according to the

Guide for the Care and Use of Laboratory Animals of the National Institutes of Health. The study was approved under the regulations of the Committee on the Ethics of Animal Experiments of Zhejiang Chinese Medical University (Permit Number: SYXK 2013-0184). Six-week-old male C57BL/6 J mice, purchased from Shanghai laboratory animal center (SLAC), were randomly divided into six groups (n = 6 per group): LFD-control group, low dose of BSGLP in LFD group (LFD-100 mg/kg), high dose of BSGLP in LFD group (LFD-300 mg/kg), HFD-control group, low dose of BSGLP in HFD group (HFD-100 mg/kg), and high dose of BSGLP in HFD group (HFD-300 mg/kg). Mice of each group were divided into two cages with 3 animals in each cage and housed in a temperature-controlled (25−28℃) specific pathogen-free environment with a 12−12 light-dark cycle. BSGLP was given to mice once a day by gavage in double distilled water solution. Control groups were given double distilled water to minimize the effects of the gavage procedure. The experiment lasted for 12 weeks during which the body weight of each mouse and food intake were monitored weekly. At the end of the trial, all the animals were euthanized by carbon dioxide. Serum was collected, epididymal white adipose tissue (eWAT), inguinal white adipose tissue (iWAT), liver, and ileum tissues were excised, weighed and part of the tissues were fixed in 4% formaldehyde. The rest of the tissues were snap-frozen in liquid nitrogen for further analysis.

2.4. Intraperitoneal glucose tolerance test (IPGTT)

IPGTT was performed at 6 and 12 weeks after the treatment of BSGLP. The mice were fasted overnight, then glucose (1.25 mg/kg) was administered by intraperitoneal injection. Tail blood samples were collected after 0, 15, 30, 60, 90, and 120 min, and blood glucose levels were determined using a glucose meter. Area under the curve (AUC) of all the linear graphs were calculated using GraphPad Prism 7 Software (La Jolla, CA, USA).

2.5. Fecal flora genomic DNA extraction

Fecal samples were collected in the last week of the experiment. Feces were collected into sterile Eppendorf tube immediately after defecation, and then snap-frozen in liquid nitrogen. Total DNA from stool bacteria was extracted using QIAamp DNA stool mini kit from Qiagen (Germantown, MD, USA) according to the manufacturer's instructions. DNA purity and concentration were determined by agarose gel electrophoresis (1 % w/v agarose) and quantified using NanoDrop 2000c spectrophotometer from Thermo Scientific (Grand Island, NY, USA).

2.6. 16 s rRNA gene amplification and sequencing

Illumina HiSeq sequencing analysis of the DNA samples was conducted by Novogene (Beijing, China). Briefly, stool bacterial DNA samples were placed in centrifuge tubes and diluted with sterile water to 1 ng/μL for each sample. 16S rRNA genes of distinct regions (16SV3-V4) were amplified using specific primers. All PCR reactions were carried out with Phusion High-Fidelity PCR Master Mix from New England Biolabs (Ipswich, MA, USA). PCR products were purified with Qiagen Gel Extraction Kit (Germantown, MD, USA). Sequencing libraries were generated using TruSeq DNA PCR-Free Sample Preparation Kit from Illumina (San Diego, CA, USA) according to standard manufacturer's recommendations. The library quality was assessed on the Qubit Fluorometer from Thermo Scientific (Waltham, MA, USA) and Agilent Bioanalyzer 2100 system. Finally, the library was sequenced on an Illumina HiSeq 2500 platform and 250 bp paired-end reads were generated.

2.7. Data analysis and bioinformatics

FLASH (Version 1.2.7) was used to splice reads of each sample to get raw tags, and the QIIME (Version 1.7.0) quality control process was used to get clean tags. These tags were compared with the reference database using UCHIME algorithm (UCHIME Algorithm) to detect chimera sequences, which were removed to obtain effective tags. Sequences with ≥ 97 % similarity were assigned to the same operational taxonomic units (OTUs) using Uparse software (Version 7.0.1001). The representative sequence for each OTU was screened for further annotation. For each representative sequence, annotation analysis was performed with RDP classifier (Version 2.2) method and the GreenGene database. Alpha diversity (Shannon index and Rank abundance) and beta diversity analysis (principal component analysis (PCA) and non-metric multidimensional scaling (NMDS)) were calculated by QIIME software (Version 1.7.0). Linear discriminant analysis (LDA) effect size (LEfSe) method was used to analyze the biomarker of intestinal flora. The alpha parameter of LEfSe test was set to 0.05, and the threshold of logarithmic score of LDA analysis was set to 4.0 to obtain a cladogram (circular hierarchical tree) showing the relationship between taxon.

2.8. Histopathological and immunohistochemical analysis

Tissues were fixed in 4 % formaldehyde and embedded in paraffin, and 4-μm sections were cut and stained with hematoxylin and eosin (H&E) for pathological analysis. ImageJ 1.41 software was used to detect the cell diameter of adipocyte as previously described (Bozec & Hannemann, 2016). A total of fifty adjacent cells from five sections of each mouse were analyzed. Data are expressed as mean adipocyte diameter (μm) from three individual mouse. The histological score (0–3) of liver steatosis was assessed using Kleiner's grading system as previously described (Kleiner et al., 2005). According to Kleiner, steatosis was scored as: 0, 0 %–5 % of the hepatocytes in the section have steatosis; 1, greater than 5 %–33 %; 2, greater than 33 %–66 %; and 3, greater than 66 % of hepatocytes have steatosis. A total of 5 fields of each section were counted, and a total of three mice were analyzed. Immunohistochemistry analysis was performed using standard methods according to the manufacturer's instructions of the primary antibody CD68 (1:500) and Claudin-1 (1:500). All images were viewed under a Nikon light microscope (Tokyo, Japan). Negative control had been performed using the secondary antibody alone. The positive area was analyzed by ImageJ 1.41 software (Bethesda, MD, USA).

2.9. RNA extraction and qRT- PCR analysis

Total RNA was isolated from tissues using Trizol reagent according to the manufacturer's instruction. The cDNAs were generated using iScript cDNA synthesis method according to the manufacturer's instruction. β-actin was used as the reference gene. The relative fold of expression change was calculated using $2^{-\Delta\Delta Ct}$ method. The mouse primers were synthesized by Life technologies and the primer sequences were listed in the Supplement (Supplementary Table S1).

2.10. Serum lipids and ELISA

After treatment with BSGLP for 12 weeks, serum was collected for detecting TC, TG, NEFA, HDL, and LDL using commercial kits. The concentration of IL-1β, IL-6, TNF-α, MCP-1, and LPS were determined by commercial ELISA kits according to the manufacturer's instructions. The concentrations of Occludin, Claudin-1, and Reg3γ in ileum tissue were also detected by ELISA and normalized by protein concentrations in ileum as determined by BCA assay.

2.11. Western blotting analysis

Total proteins were lysed in ice-cold RIPA buffer containing phosphatase inhibitors. Protein concentration was determined by BCA protein assay kit. The total protein (40 μg) was resolved by SDS PAGE gel and then transferred to PVDF membrane. After blocking with 5 % skim milk in TBST at room temperature for 1 h, the membranes were probed

overnight at 4 °C with primary antibodies (1:1000) and then HRP-conjugated secondary antibody (1:2000) according to manufacturer's instructions. The signals were captured using western lightning Plus ECL enhanced chemiluminescence substrate. ImageJ 1.41 software was used for the quantitative analysis of optical density. A total of three samples from each group were selected to represent three repeats.

2.12. Measurements of fecal SCFAs

The quantification analysis of fecal SCFAs was determined by gas chromatography-mass spectrometry (GC–MS) using Agilent 7890A/5975C conducted by Bionovogene Co. Ltd (Suzhou, Jiangsu, China). Briefly, 100 mg sample was weighed and mixed with 1 mL 0.005 M NaOH solution and 50 μL 2-methyl-butyric acid for 2 min and incubated at 4℃ for 2 h. Next, the mixture was mixed for 2 min and centrifuged for 20 min (4 ℃ at 13,000 rpm). 500 μL supernatant was transferred to a clean tube, then added with 300 μL distilled water, 500 μL isopropanol/pyridine solution (3:2, v/v) and platelet cytotoxic factor solution for derivatization, and then extracted with 500 μL n-hexane for analysis. Agilent HP-5 capillary column (30 m*0.25 mm*0.25 μm) was used for chromatographic separation. Samples were injected with a split ratio of 10:1, and a 1 μL injected volume. The temperature of inlet, ion source, and transfer line were 280℃, 230℃, and 250℃. Program heating initial temperature was 60℃ and incubated for 5 min, then raise the temperature to 250℃ at 10℃/min. The helium carrier flow rate was 1.0 mL/min. Data handing was performed with an Agilent's MSD ChemStation (E.02.00.493, Agilent Technologies, Inc., USA).

2.13. Fecal microbiota transplantation (FMT)

In the FMT study, the microbiota donor mice were treated with HFD or HFD and 300 mg/kg of BSGLP for 6 weeks, then followed by daily collection of feces. Feces from each group were pooled, and 200 mg was resuspended in 2 mL of sterile saline. The mixture was vigorously vortexed for 10 s before centrifugation at 800 *g* for 3 min. The supernatant was collected and used as transplant material. Meanwhile, eight-week-old male C57BL/6 J mice were randomly divided into three groups (7 mice/group). After acclimation for 2 weeks, mice were treated with the antibiotics cocktail (ampicillin, 1 g/L; metronidazole, 1 g/L; vancomycin, 0.5 g/L; neomycin, 0.5 g/L) in drinking water for 1 week to create the pseudo germ-free mice. The germ-free mice were oral gavaged with fecal suspension (150 μL) from mice with HFD or HFD and 300 mg/kg BSGLP once a day for 6 weeks and supplied with HFD diet. The body weight was monitored weekly and blood samples were collected at the end of the experiment for analysis of inflammatory factors.

2.14. Statistical analysis

GraphPad Prism 7 was used for all statistical analyses. Data are shown as mean ± SEM (standard error of the mean). All experiments were repeated three times, except for the FMT, SCFAs measurement, 16 s rRNA gene amplification and sequencing experiments. Difference between pairwise groups was tested for statistical significance by student's *t*-test, while one-way or two-way ANOVA with post hoc Bonferroni's correction was used for multiple comparisons. In addition, the analysis of datasets containing multiple measurements from each mouse with one-way or two-way ANOVA for repeated measurements were corrected using the false discovery rate approach of Benjamini-Hochberg method with q-value 0.05. A value of $P < 0.05$, was considered to be statistically significant.

3. Results

3.1. BSGLP inhibits HFD-induced body weight increase, fat accumulation, and hyperlipidemia in mice

After feeding with HFD for 12 weeks, body weight was significantly increased in C57BL/6 J mice compared with LFD-fed mice (Fig. 1A, B). Both doses of BSGLP significantly inhibited body weight increase and final weight gain under HFD from week 9 to week 12 (Fig. 1A, B). There was no significant change in food intake among all groups upon both diets (Supplementary Fig. S1A, B). Besides, both doses of BSGLP significantly attenuated the excessive fat accumulation in eWAT and iWAT upon HFD (Fig. 1C, D), accompanied by an increase in the size of adipocytes as compared to LFD treatment (Fig. 1E, F). After quantification, the cell diameter of adipocyte was significantly increased by HFD compared with LFD treatment in eWAT and iWAT (Fig. 1E, F). However, consistent with the effects on body weight, the treatment of BSGLP significantly reduced the cell diameter of adipocytes in both adipose tissues (Fig. 1E, F). Moreover, HFD significantly increased the weight of liver tissue and induced hepatic steatosis, while BSGLP treatment inhibited HFD-induced fat accumulation and steatosis in liver (Supplementary Fig. S1C–E).

Hyperlipidemia is usually induced by HFD, which is a serious risk factor for metabolism-related diseases. We found that HFD significantly increased serum levels of TC and LDL in mice, which were reversed upon BSGLP treatment (Fig. 1G). Surprisingly, we did not observe a significant change of TG upon HFD treatment, which has also been reported before (Eisinger et al., 2014), while BSGLP may have a tendency to reduce serum TG (Fig. 1G). In addition, we found that HDL was significantly increased upon HFD treatment, which has also been reported by others (Hayek et al., 1993), while BSGLP had no effects on HDL expression upon both diets (Fig. 1G). In LFD groups, we found high dose of BSGLP reduced serum level of NEFA, while in HFD groups both doses of BSGLP significantly reduced NEFA (Fig. 1G). Unfortunately, we didn't find improvement in HFD-induced fasting hyperglycemia and glucose intolerance by BSGLP treatment (Supplementary Fig. S2A–F). Taken together, these data suggest that BSGLP significantly reduced HFD-induced body weight increase, fat accumulation in adipose tissues, hepatic steatosis, and hyperlipidemia at a certain degree in C57BL/6 J mice.

3.2. BSGLP inhibits HFD-induced inflammation

Chronic low-grade inflammation is one of the most important characteristics of obesity (Maurizi, Della Guardia, Maurizi, & Poloni, 2018). In order to evaluate the anti-inflammation effect of BSGLP, we examined the serum levels of pro-inflammatory cytokines including TNF-α, IL-1β, IL-6, and MCP-1 in mice. As shown in Fig. 2A, HFD significantly increased TNF-α and IL-1β in serum but did not change IL-6 and MCP-1 levels. Under HFD, BSGLP at both concentrations significantly reduced serum levels of TNF-α, IL-1β, and MCP-1 compared with HFD-control alone (Fig. 2A). Moreover, HFD significantly increased the mRNA expression of *TNF-α, IL-1β, IL-6*, and *MCP-1* in eWAT (Fig. 2B). On the contrary, the expressions of these pro-inflammatory cytokines (*IL-1β, IL-6*, and *MCP-1*) were significantly reduced by the intervention of 300 mg/kg BSGLP (Fig. 2B).

3.3. BSGLP inhibits HFD-induced macrophage infiltration in eWAT

As in obesity condition, macrophages infiltrate into WAT and release inflammatory cytokines (Maurizi et al., 2018), we then examined the mRNA expression of *CD11b, CD11c,* and *CD68*, key markers of macrophage infiltration. The results showed that HFD significantly increased these factors in eWAT, while both doses of BSGLP significantly reduced the expression of these macrophage infiltration markers except the effect of 300 mg/kg of BSGLP on *CD11b* (Fig. 3A). In addition, IHC analysis

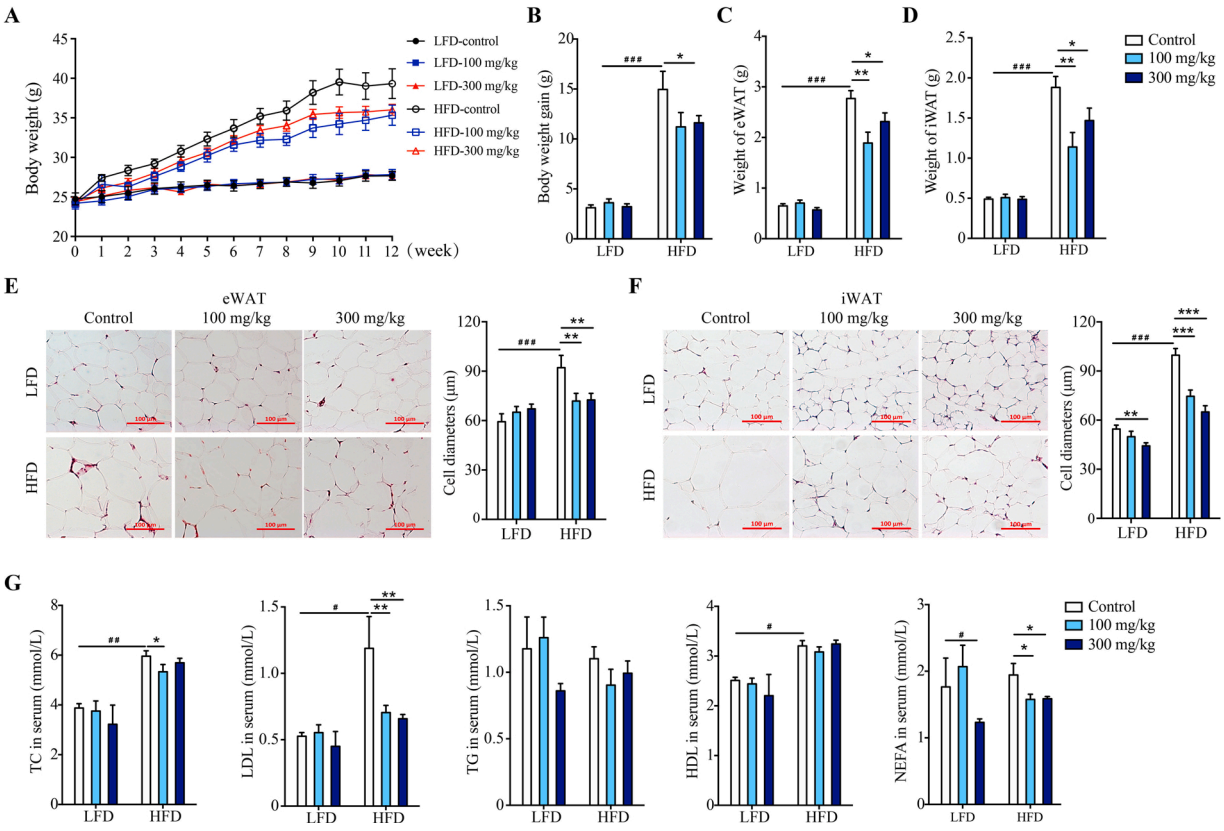

Fig. 1. BSGLP attenuates fat accumulation and hyperlipidemia in HFD-fed mice. (A) Body weight of mice after the treatment of BSGLP upon LFD and HFD for 12 weeks. (B) Body weight gain. (C) Weight of eWAT. (D) Weight of iWAT. (E) Representative H&E staining images of eWAT (scale bar, 100 μm) and cell diameter of adipocytes. (F) Representative H&E staining images of iWAT (scale bar, 100 μm) and relative cell diameter of adipocytes. (G) Levels of total cholesterol (TC), triacylglycerol (TG), high-density lipoprotein (HDL), low-density lipoprotein (LDL), and non-esterified fatty acid (NEFA) in the serum of mice. Data are shown as means ± SEM (n = 6 mice/group). Statistical analysis was performed using two-way ANOVA followed by Benjamini-Hochberg method for the false discovery rate correction. $^{\#}P < 0.05$, $^{\#\#}P < 0.01$, $^{\#\#\#}P < 0.001$ when comparing LFD-control with HFD-control, $^{*}P < 0.05$, $^{**}P < 0.01$, $^{***}P < 0.001$ when comparing BSGLP intervention group with control group under the same diet.

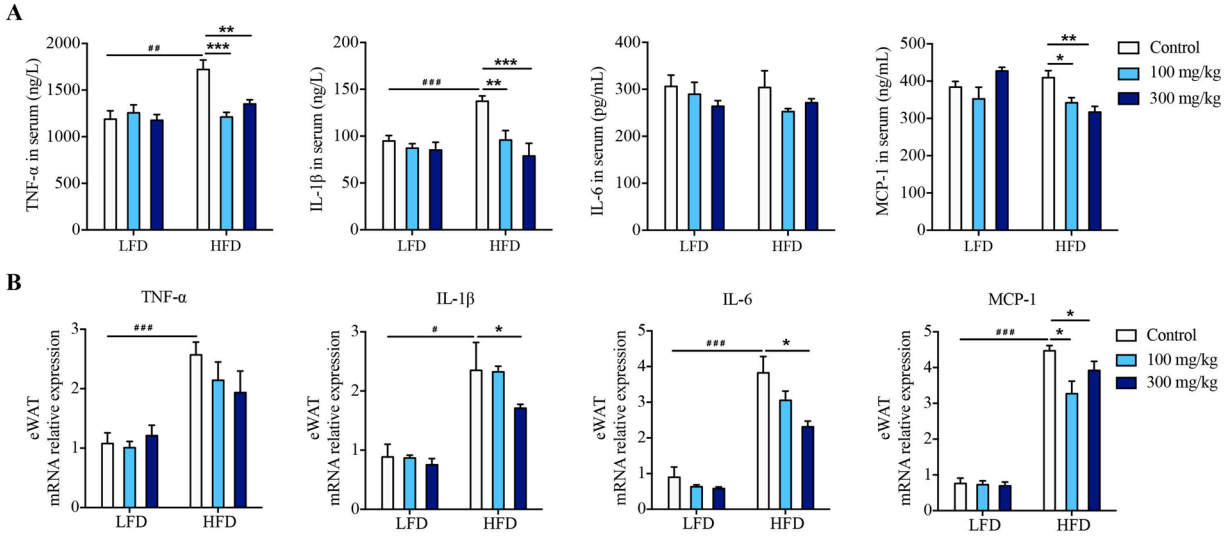

Fig. 2. BSGLP inhibits the expression of proinflammatory cytokines in HFD-fed mice. (A) Serum protein levels of TNF-a, IL-1β, IL-6, and MCP-1 were determined by ELISA. (B) Relative mRNA expression of *TNF-α*, *IL-1β*, *IL-6*, and *MCP-1* in eWAT as determined by qRT-PCR. Data are shown as means ± SEM (n = 6 mice/group). Statistical analysis was performed using two-way ANOVA followed by Benjamini-Hochberg method for the false discovery rate correction. $^{\#}P < 0.05$, $^{\#\#}P < 0.01$, $^{\#\#\#}P < 0.001$ when comparing LFD-control with HFD-control, $^{*}P < 0.05$, $^{**}P < 0.01$, $^{***}P < 0.001$ when comparing BSGLP intervention group with control group under HFD.

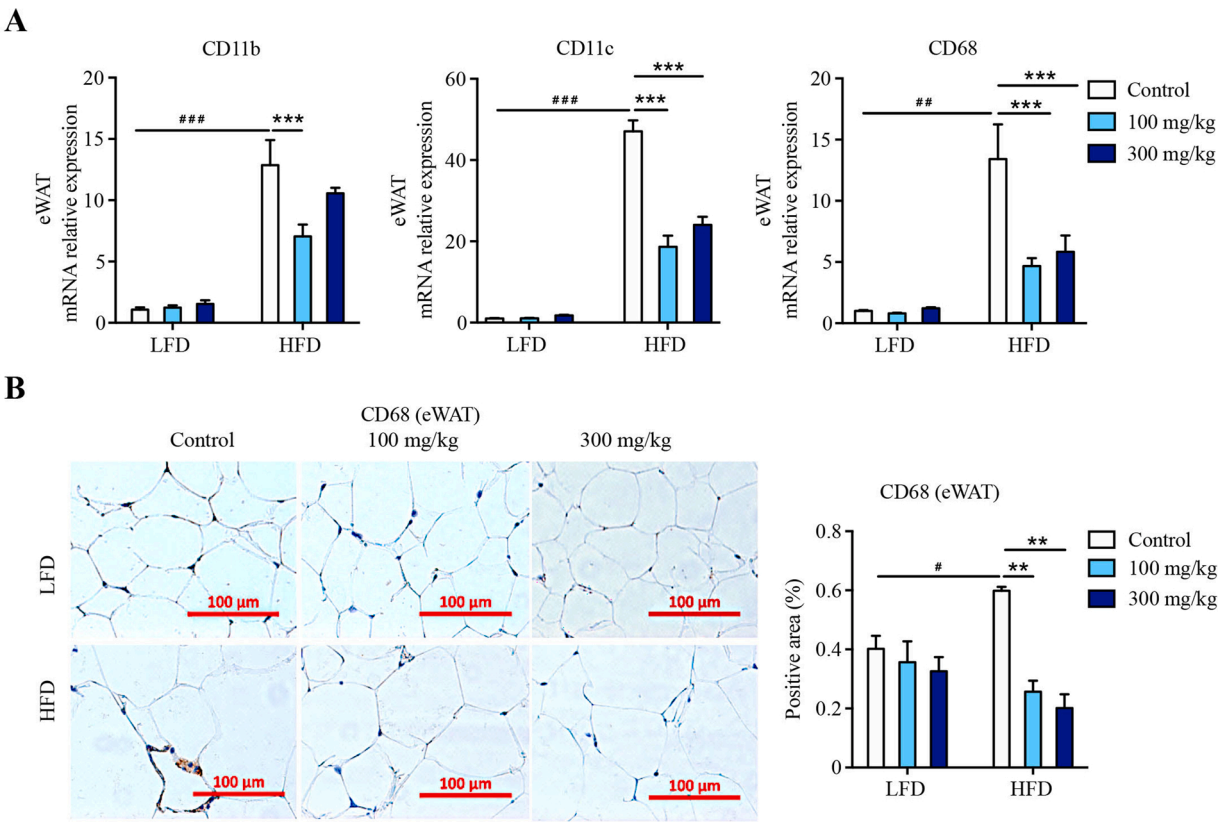

Fig. 3. BSGLP inhibits macrophage infiltration in eWAT in HFD-fed mice. (A) Relative mRNA expression of *CD11b*, *CD11c*, and *CD68* in eWAT as determined by qRT-PCR. (B) Representative immunohistochemistry images and quantification of CD68 in eWAT, scale bar, 100 μm. Data are shown as means ± SEM (n = 6 mice/group). Statistical analysis was performed using two-way ANOVA followed by Benjamini-Hochberg method for the false discovery rate correction. $^{\#}P < 0.05$, $^{\#\#}P < 0.01$, $^{\#\#\#}P < 0.001$ when comparing LFD-control with HFD-control, $^{**}P < 0.01$, $^{***}P < 0.001$ when comparing BSGLP intervention group with control group under HFD.

further confirmed that both doses of BSGLP significantly decreased HFD-induced macrophage infiltration as evidenced by reduced CD68 staining in eWAT (Fig. 3B).

3.4. BSGLP changes the overall structure of gut microbiota

To analyze the effect of BSGLP on the composition of gut microbiota, pyrosequencing-based analysis of bacterial 16 s rRNA (V3-V4 region) in mice feces was performed. LFD treatments were included to differentiate effects on microbiota composition by body weight change or BSGLP alone. Shannon index and Rank abundance curves indicated that the sequencing depth covered rare new phylotypes and most of the diversity (Supplementary Fig. S3A, B). PCA analysis showed distinct clustering of microbiota composition for each group (Fig. 4A). PC1 showed 15.59 % difference which mainly reflected the impact of LFD and HFD on the structural changes of the gut microbiota (Fig. 4A). Ordinate PC2 showed 7.14 % of the total variance which mainly reflected the effect of BSGLP on the gut microbiota (Fig. 4A). The NMDS plot of the microbial compositions of the 36 samples revealed that the BSGLP treatment groups and control groups have obviously different microbiome compositions (Fig. 4B). These results indicate that other than HFD, BSGLP also plays an important role in regulating the profile of gut microbiota. As shown in Fig. 4C, the main phyla observed in our study include *Firmicutes, Bacteroidetes, Proteobacteria, Actinobacteria, Verrucomicrobia, Tenericutes, Deferribacteres*, and *Saccharibacteria*. Consistent with previous studies (Chang et al., 2015; Chen, Li, Liu, Liu, & Han, 2018), HFD significantly changed the composition of gut microbiota by increasing the *Firmicutes/Bacteroidetes* ratio (Fig. 4D). BSGLP at 300 mg/kg showed a tendency to reduce the *Firmicutes/Bacteroidetes* ratio under HFD at a non-significant level (Fig. 4D).

3.5. BSGLP improves HFD-induced gut microbiota disorder at genus and species levels

Next, we studied the specific changes in the gut microbiota at the genus level upon HFD and BSGLP treatments. The most abundant bacteria mainly include *Allobaculum*, *Desulfovibrio*, *Lachnospiraceae_NK4A136_group*, *Blautia*, *Helicobacter*, *Bacteroides*, *Ruminiclostridium_9*, *Coriobacteriaceae_UCG-002*, *Lactobacillus*, and *Alloprevotella* (Supplementary Fig. S3C). Detailed analysis at genus level revealed that HFD feeding significantly upregulated or downregulated the relative abundance of a number of bacteria (Fig. 5A). Particularly, HFD significantly decreased the relative abundance of *Allobaculum*, *Coriobacteriaceae_UCG-002*, *Akkermansia*, *Bifidobacterium*, *Turicibacter*, *Parabacteroides*, *Ruminococcaceae_UCG-010*, and *Christensenellaceae_R-7_group* (Fig. 5A), while significantly increased the relative abundance of *Blautia*, *Rikenella*, *Ruminiclostridium_UGC-009*, *Lachnospiraceae_FCS020_group*, *Lachnospiraceae_UCG-001*, and *Lachnospiraceae_UCG-005* (Fig. 5A). Under HFD, the intervention of BSGLP reversed the abundance of these bacteria, in particular, the potential probiotics including *Allobaculum*, *Bifidobacterium*, and *Christensenellaceae_R-7_group* which have been reported positively related with anti-obesity (Fig. 5A) (Liu et al., 2019; Wang, Tang et al., 2015; Zhang et al., 2015). In addition, we found that upon LFD, BSGLP significantly increased the abundance of *Allobaculum* and *Bifidobacterium*, and decreased the abundance of *Lachnospiraceae_UCG-001* and *Ruminiclostrdium* at the genus level (Fig. 5A). Fig. 5B is the representative graph of several bacteria that were changed by HFD and BSGLP treatments at the genus level. These data suggest that BSGLP can shape the profile of gut microbiota with or without the intervention of HFD in mice.

Moreover, at the species level, we found that the abundance of a number of bacteria was significantly changed upon HFD and BSGLP

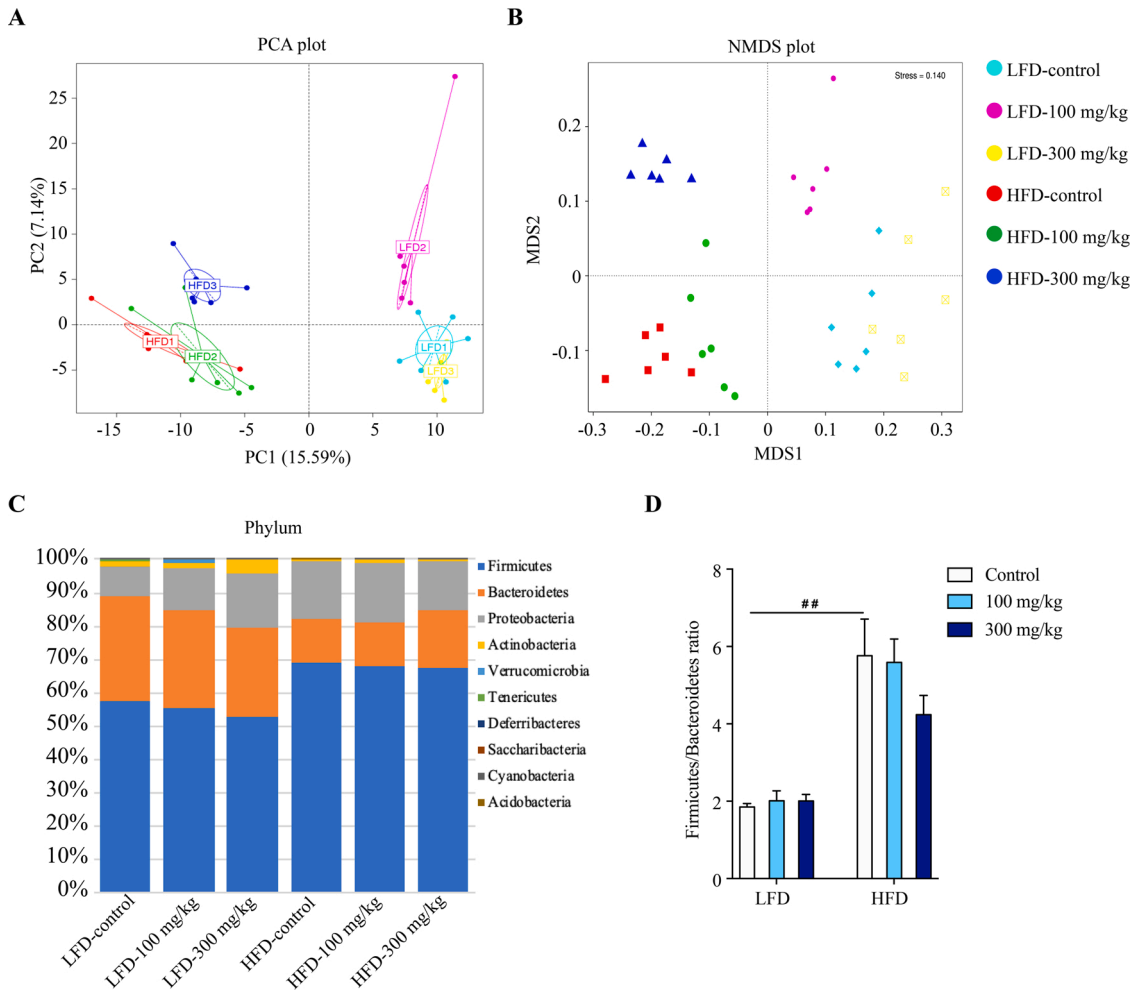

Fig. 4. BSGLP modulates the composition of gut microbiota. (A) Principal component analysis (PCA) of gut microbiota between six groups. (B) Non-metric multidimensional scaling (NMDS) analysis of the gut microbiota. (C) The relative abundance of the top ten abundant bacteria at the phylum level. (D) The ratio of Firmicutes/Bacteroides. Data are shown as means ± SEM (n = 6 mice/group). Statistical analysis was performed using two-way ANOVA followed by Benjamini-Hochberg method for the false discovery rate correction. $^{\#\#}P < 0.01$ when comparing LFD-control with HFD-control.

treatment (Fig. 6A). For example, the probiotics *Bifidobacterium_choerinum* was significantly decreased and *Bacteroides_chinchillae* was slightly reduced by HFD (Fig. 6A). However, their abundances were highly induced by the treatment of BSGLP at different levels (Fig. 6A). In addition, HFD also significantly increased *Firmicutes_bacterium_ASF500*, *Alistipes_*sp._*627*, and *Clostridium_leptum*, which were significantly reduced by the treatment of BSGLP upon HFD (Fig. 6A). Upon LFD treatment, BSGLP could also significantly increased or decreased the abundance of certain microbiota at species level, including increasing *Bifidobacterium_choerinum* and *Bacteroides_chinchillae,* and decrease *Firmicutes_bacterium_ASF500* (Fig. 6A). Fig. 6B is the representative graph of several bacteria that were changed by HFD and BSGLP treatments at the species level.

Next, LEfSe analysis was performed to identify fecal microbial taxa that accounted for the greatest differences among all the groups. Our results indicated that there were 6, 0, 9, 12, 6, and 12 significant differences in the LFD-control, LFD-100 mg/kg, LFD-300 mg/kg, HFD-control, HFD-100 mg/kg, and HFD-300 mg/kg groups, respectively (Fig. 6C). The marker taxa of different levels among the experimental groups obtained from the LEfSe also supported by cladograms analysis (Fig. 6D). Overall, these results further demonstrate that BSGLP has a role in shaping the gut microbiota with or without the intervention of HFD in mice.

3.6. BSGLP increases SCFAs level and activates GPR43 in eWAT

It is known that SCFAs are the end products that are fermented from dietary fibers and indigestible polysaccharides by gut microbiota (Makki et al., 2018). Such as butyrate acts as an important energy source for colonic epithelial cells, while acetate and propionate can reach target organs where they elicit biological functions, including serving as substrates for glucogenesis (Canfora, Jocken, & Blaak, 2015; Makki et al., 2018). Next, we examined concentrations of SCFAs in feces. We found significantly reduced butyrate in HFD-induced obese mice and was reversed by both doses of BSGLP (Fig. 6E). We also found 300 mg/kg BSGLP significantly increased acetate in HFD-induced obese mice (Fig. 6E). However, there were no differences in fecal propionate and valerate levels in all treatment groups. Taken together, the treatment of BSGLP can increase SCFAs, in particular acetate and butyrate production, in HFD-fed obese mice.

Recently, some studies reported that SFCAs modulate the immune response in intestinal epithelial cells or neutrophils dependent on the sensing receptors, G-protein coupled receptor 41 (GPR41) or GPR43 (Kim, Kang, Park, Yanagisawa, & Kim, 2013). Outside of the ileum, SFCAs-GPR41/43 also play an important role in adipose tissue (Kimura et al., 2013). While the effect of GLP on GPR41/43 has never been reported before. Therefore, we detected the expression of GPR41/43 in the ileum and eWAT. However, no significant changes were observed in the expression of GRP41 at both the mRNA and protein levels in our study

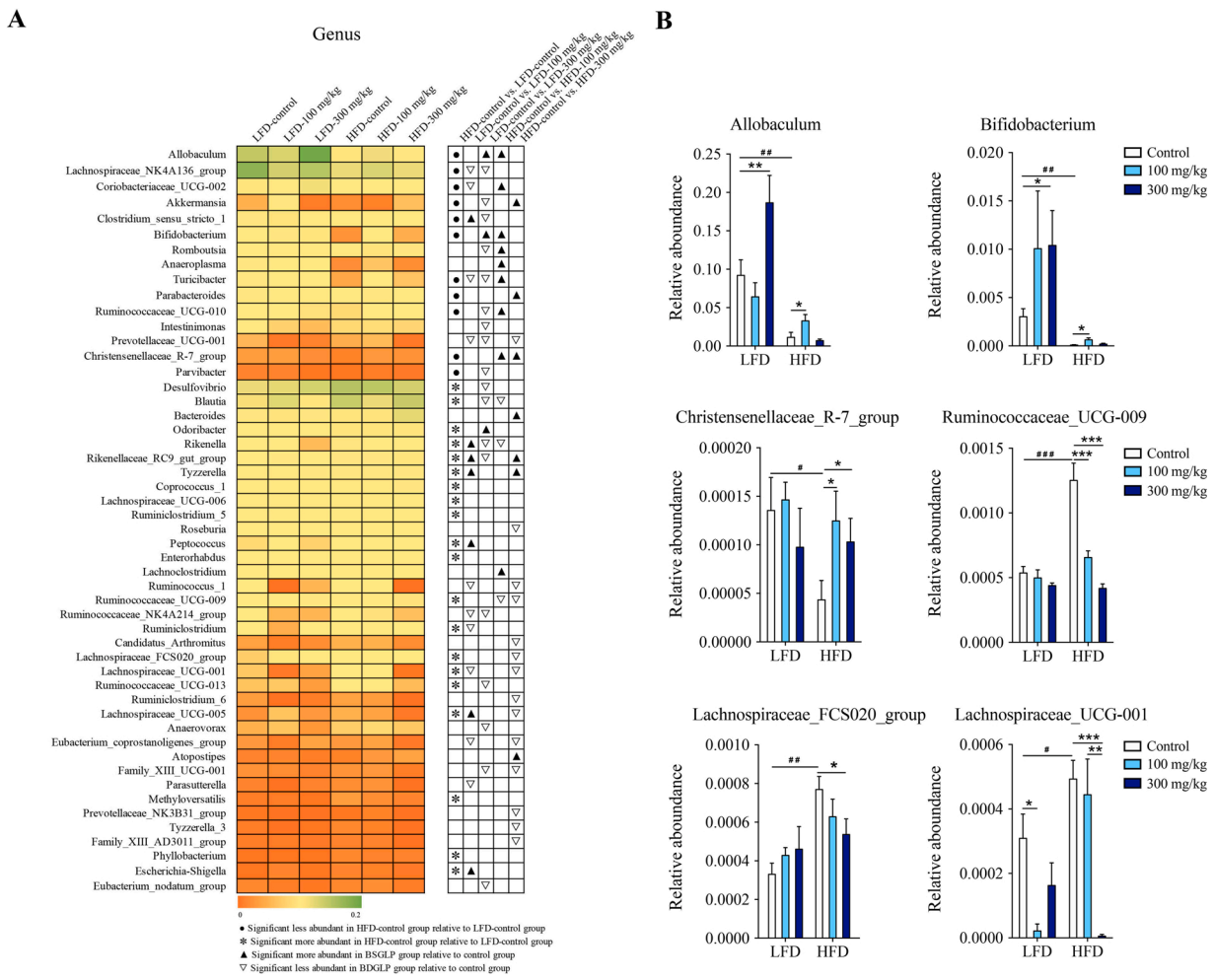

Fig. 5. Deep analysis of gut microbiota at genus level in mice. (A) Bacterial genus significantly changed by HFD and the treatment of BSGLP. (B) Representative histogram of the gut microbiota at the genus level. Data are shown as means ± SEM (n = 6 mice/group). Statistical analysis was performed using two-way ANOVA followed by Benjamini-Hochberg method for the false discovery rate correction. $^{\#}P < 0.05$, $^{\#\#}P < 0.01$, $^{\#\#\#}P < 0.001$ when comparing LFD-control with HFD-control, $^{*}P < 0.05$, $^{**}P < 0.01$, $^{***}P < 0.001$ when comparing BSGLP intervention group with control group under the same diet.

(data not shown). We next examined whether GRP43 plays an important role in the BSGLP mediated biological effects. We found no significant changes of GPR43 expression in the ileum at both the mRNA and protein levels (Fig. 6F, G). However, the mRNA and protein expressions of GPR43 in eWAT were significantly decreased upon HFD compared with LFD, and the reduction of GPR43 expression by HFD was significantly reversed by both doses of BSGLP treatment (Fig. 6F, G). Under LFD, the low dose of BSGLP significantly increased GPR43 expression (Fig. 6G). Our results suggest that BSGLP may regulate metabolism and inhibit obesity by activating GPR43 in adipose tissues in response to the change of gut microbiota composition and the increased production of SCFAs.

3.7. BSGLP improves endotoxemia and gut barrier function

It has been well established that disordered gut microbiota can disrupt the integrity of enterocyte tight junction, which would lead to LPS flow into the bloodstream and cause systemic inflammation (Winer, Luck, Tsai, & Winer, 2016; Zhao, 2013). We first examined the level of serum LPS by ELISA and found it was significantly increased by HFD, while both doses of BSGLP significantly down-regulated LPS level (Fig. 7A). We then determined the expression of the tight junction proteins, Occludin, Claudin-1, and ZO-1 in ileum using multiple methods. As shown in Fig. 7B, HFD significantly reduced the expression of Claudin-1 protein in ileum as determined by ELISA, and this reduction was significantly reversed by both doses of BSGLP. Although HFD did not have an effect on Occludin expression in ileum as determined by ELISA, both doses of BSGLP significantly increased the level of this protein in ileum upon HFD (Fig. 7B). IHC staining revealed that Claudin-1 expression in the ileum was dramatically reduced by HFD, while both doses of BSGLP significantly induced Claudin-1 expression upon HFD after quantification analysis (Fig. 7C). Western blotting analysis further demonstrated that the expression of Occludin and ZO-1 were significantly reduced in the ileum by HFD, while BSGLP treatment increased their expression at certain degree upon both diets (Fig. 7D–F). Meanwhile, there were no much effects on the mRNA expression of *ZO-1* and *Claudin-1* among all groups (Supplementary Fig. S4A).

Furthermore, we examined the expression of antimicrobial peptides (Lyz1 and Reg3γ), as they are the main components of the innate immune system of the gut (Kurashima & Kiyono, 2017). Our results showed that Lyz1 and Reg3γ expressions were significantly decreased by HFD in ileum at the protein level as determined by Western blotting (Fig. 7D, G) or ELISA (Fig. 7 H), respectively. Interestingly, the reduction of Lyz1 and Reg3γ expressions induced by HFD were reversed at a certain point by BSGLP treatment (Fig. 7D, G, H). At the mRNA level, 100 mg/kg of BSGLP significantly increased HFD-induced *Reg3γ* downregulation (Supplementary Fig. S4B), but both HFD and BSGLP had no effects on *Lyz1* expression in the ileum (data not shown). Taken together, these results indicate that BSGLP has a beneficial effect on improving the gut barrier function evidenced by increased expressions of tight junction proteins and antimicrobial peptides.

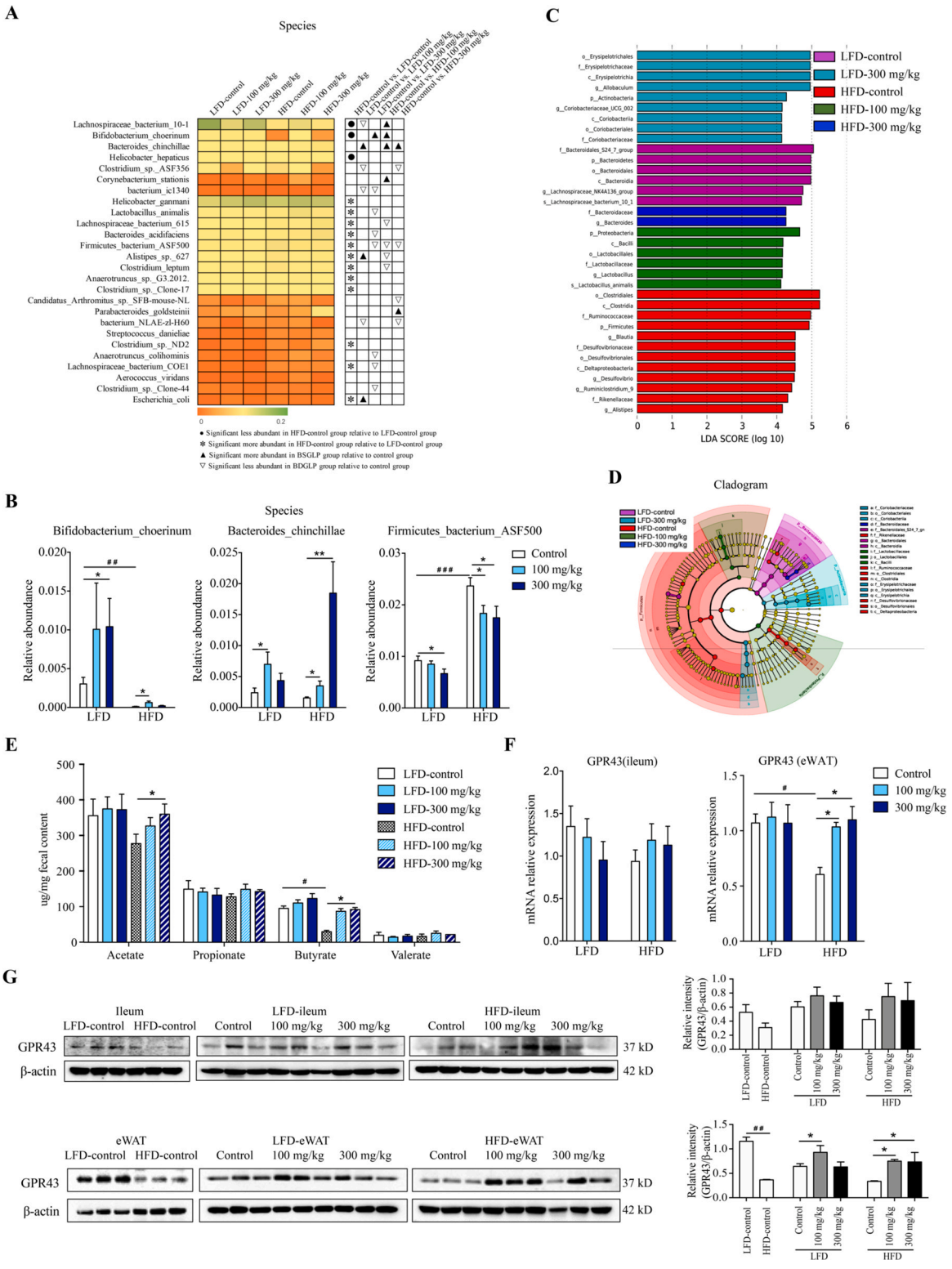

Fig. 6. Deep analysis of gut microbiota at species level and the effects of BSGLP on SCFAs level and GPR43 expression. (A) Analysis of significantly changed bacterial species upon HFD and BSGLP treatment. (B) Representative histogram of the gut microbiota at the species level. (C) Linear discriminate analysis effect size (LEfSe) analysis of the dominant biomarker taxa among the six groups. The threshold of the logarithmic score of LDA analysis was 4.0. (D) Taxonomic cladogram obtained from LEfSe analysis by comparing 6 groups. (E) The effect of BSGLP on the fecal level of SCFAs. (F) GPR43 mRNA expression in ileum and adipose tissue as determined by qRT-PCR. (G) GPR43 expression in ileum and adipose tissue as determined by Western blotting. Data are presented as means ± SEM. Two-way ANOVA followed by Benjamini-Hochberg method for the false discovery rate correction in Figure A-F, n = 6 mice/group. Student's unpaired *t*-test and one-way ANOVA followed by Benjamini-Hochberg method for the false discovery rate correction in Figure G, n = 3 mice/group. $^{\#}P < 0.05$, $^{\#\#}P < 0.01$, $^{\#\#\#}P < 0.001$ when comparing LFD-control with HFD-control, $^{*}P < 0.05$, $^{**}P < 0.01$ when comparing BSGLP intervention group with control group under the same diet.

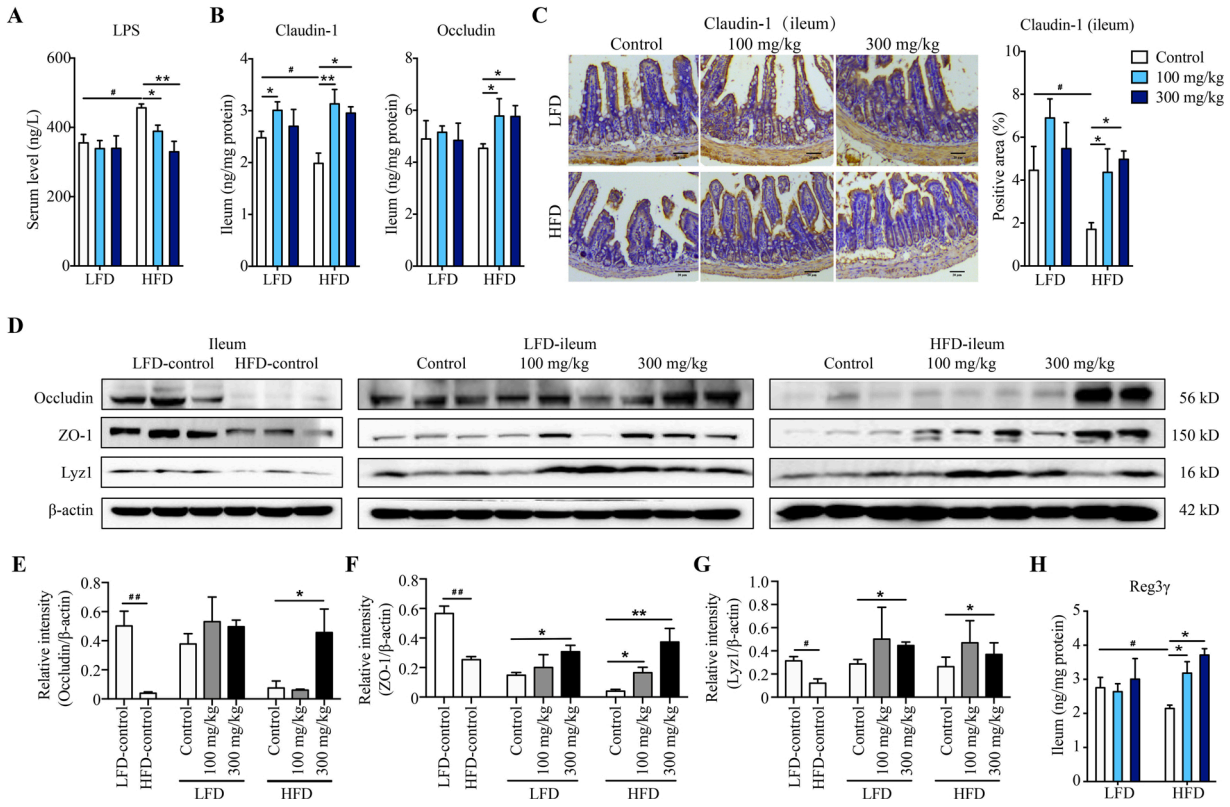

Fig. 7. BSGLP ameliorates endotoxemia and enhances gut barrier function in HFD-fed mice. (A) Serum level of LPS as determined by ELISA. (B) Ileum level of Claudin-1 and Occludin protein expression as determined by ELISA. (C) Representative immunohistochemistry images and quantification of Claudin-1 in the ileum, scale bar, 20 μm. (D) Western blotting results of Occludin, ZO-1, and Lyz1 protein expression in the ileum. (E–G) The relative intensities of Occludin (E), ZO-1 (F), and Lyz1 (G) were calculated after normalization against β-actin. (H) The protein level of Reg3γ in the ileum as determined by ELISA. Data are shown as means ± SEM. Two-way ANOVA followed by Benjamini-Hochberg method for the false discovery rate correction was performed in Figure A–C and H (n = 6 mice/group). Student's unpaired *t*-test and one-way ANOVA followed by Benjamini-Hochberg method for the false discovery rate correction was performed in Figure E–G, (n = 3 mice/group). $^{\#}P < 0.05$, $^{\#\#}P < 0.01$ when comparing LFD-control with HFD-control, $^{*}P < 0.05$, $^{**}P < 0.01$ when comparing BSGLP intervention group with control group under the same diet.

3.8. BSGLP inhibits LPS/TLR4/NF-κB signaling pathway

It has been well established that TLR4 can recognize LPS and activate NF-κB to regulate the production of pro-inflammatory cytokines such as TNF-α and IL-1β (Zhao, 2013). We next examined the expression changes of related genes of this pathway in eWAT. Consistent with the level of LPS above, HFD significantly increased mRNA expression of *LBP*, *CD14*, *TLR4*, and *Myd88* (Fig. 8A). Notably, BSGLP significantly reduced HFD-induced induction of the expression of *LBP*, *CD14*, and *Myd88* (Fig. 8A). Moreover, Western blotting revealed that TLR4 and Myd88 protein expressions were significantly increased upon HFD (Fig. 8B–D), while p-NF-κB slightly increased by HFD compared with LFD (Fig. 8B, E). The treatment of 300 mg/kg BSGLP significantly reduced the expression of TLR4 and Myd88 in HFD-fed mice (Fig. 8B–D), and both doses of BSGLP significantly decreased the expression of p-NF-κB upon both diets (Fig. 8B, E). These results suggest that BSGLP may inhibit HFD-induced inflammatory response through inhibition of the TLR4/NF-κB signaling pathway.

3.9. Gut microbiota mediates the beneficial effects of BSGLP on obesity

In order to investigate whether the anti-obesity and anti-inflammation effects of BSGLP depend on the microbiota, we performed an FMT experiment in pseudo germ-free mice. First, the antibiotics were used to remove gut microbiota to obtain the pseudo germ-free recipient mice. After transplanted with microbiota from mice fed with HFD or HFD with 300 mg/kg BSGLP, the recipient mice were fed with HFD diet for 6 weeks (Fig. 9A). As a result, the mice received microbiota from HFD with BSGLP group showed significantly lower body weight gain, eWAT weight, and iWAT weight compared with mice received microbiota from HFD (Fig. 9 C, D). However, there was no significant effect on the weight of liver (Fig. 9 D). Furthermore, FMT from HFD with BSGLP significantly reduced serum level of LPS and TNF-α, and slightly reduced IL-1β and MCP-1 concentrations in serum at nonsignificant level (Fig. 9 E). These results showed that the beneficial effects of BSGLP could be transmitted by fecal transplantation, indicating that the weight loss and inflammation-regulating effects of BSGLP were at least partially dependent on the gut microbiota.

4. Discussion

Obesity is a huge global burden and health hazard, which has few effective treatments at present. Recent evidence suggests that the occurrence of obesity is closely related to alteration in the gut microbiome. Diet, on the other hand, could deeply alter the gut microbiota composition, and thus growing interests have been aimed to modulate gut microbiota as a therapeutic strategy against obesity and its related diseases. Many studies have found that bioactive components of natural products, including berberine, *Rhizoma Atractylodis*, *Ophiopogon*, *Hirsutella sinensis*, and *G. lucidum*, can inhibit the development of obesity in experimental animals by regulating gut microbiota (Chang et al., 2015; Chen et al., 2018; Wang, Bose, Kim, Han, & Kim, 2015; Wu et al., 2019; Zhang et al., 2015). Although previous studies have shown that mycelium of *G. lucidum* has beneficial effects in obese mice related to its regulation of gut microbiota (Chang et al., 2015; Xu et al., 2017), the anti-obesity effect, and modulation of gut microbiota of GLP extracted

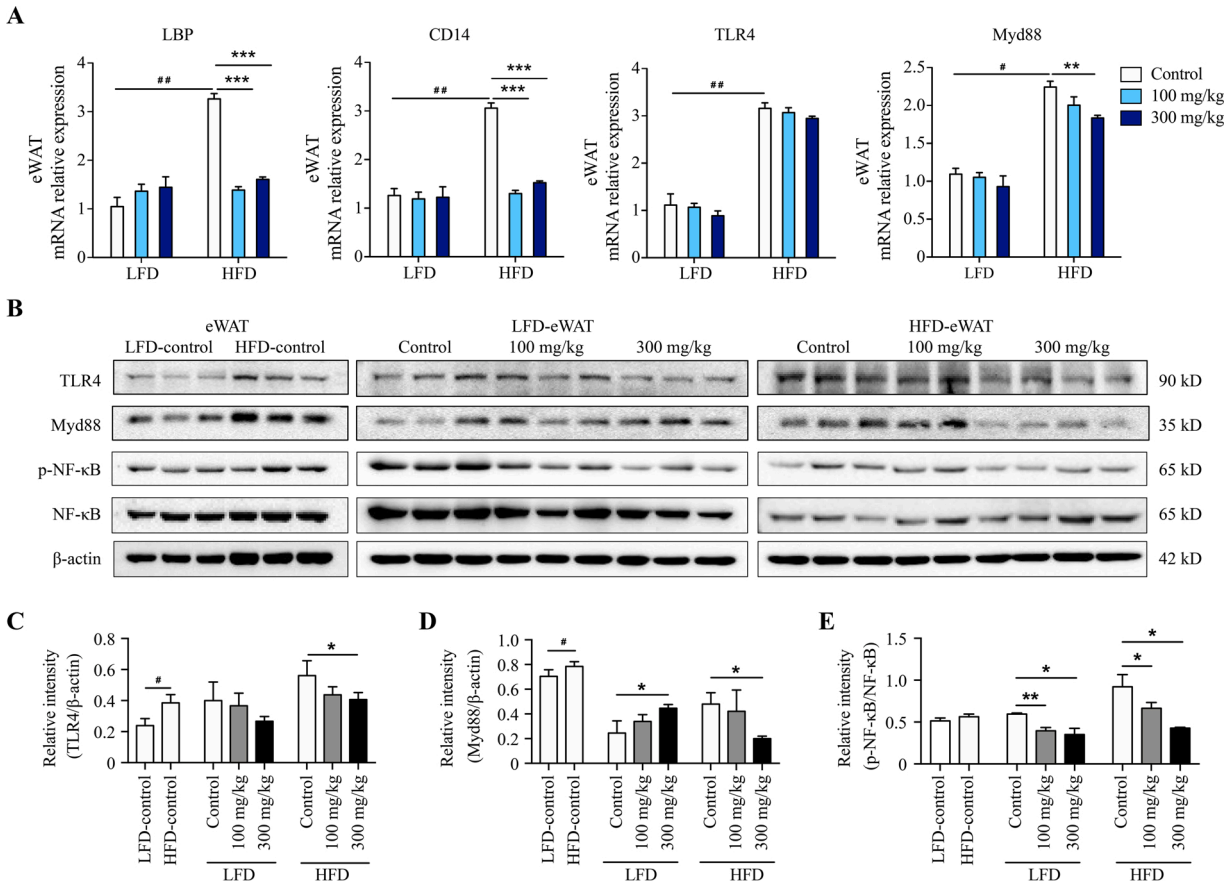

Fig. 8. BSGLP down-regulated the TLR4/NF-κB pathway in eWAT in HFD-fed mice. (A) Relative mRNA expression of *LBP*, *CD14*, *TLR4*, and *Myd88* in eWAT as determined by qRT-PCR. (B) Western Blotting results of TLR4, Myd88, and p-NF-κB protein expression in eWAT. (C–E) The relative intensities of proteins were calculated after normalization against β-actin or NF-κB. Data are shown as means ± SEM. Two-way ANOVA followed by Benjamini-Hochberg method for the false discovery rate correction was performed in Figure A (n = 6 mice/group). Student's unpaired *t*-test and one-way ANOVA followed by Benjamini-Hochberg method for the false discovery rate correction was performed in Figure C–E, (n = 3 mice/group). $^{\#}P < 0.05$, $^{\#\#}P < 0.01$ when comparing LFD-control with HFD-control, $^{*}P < 0.05$, $^{**}P < 0.01$, $^{***}P < 0.001$ when comparing BSGLP intervention group with control group under the same diet.

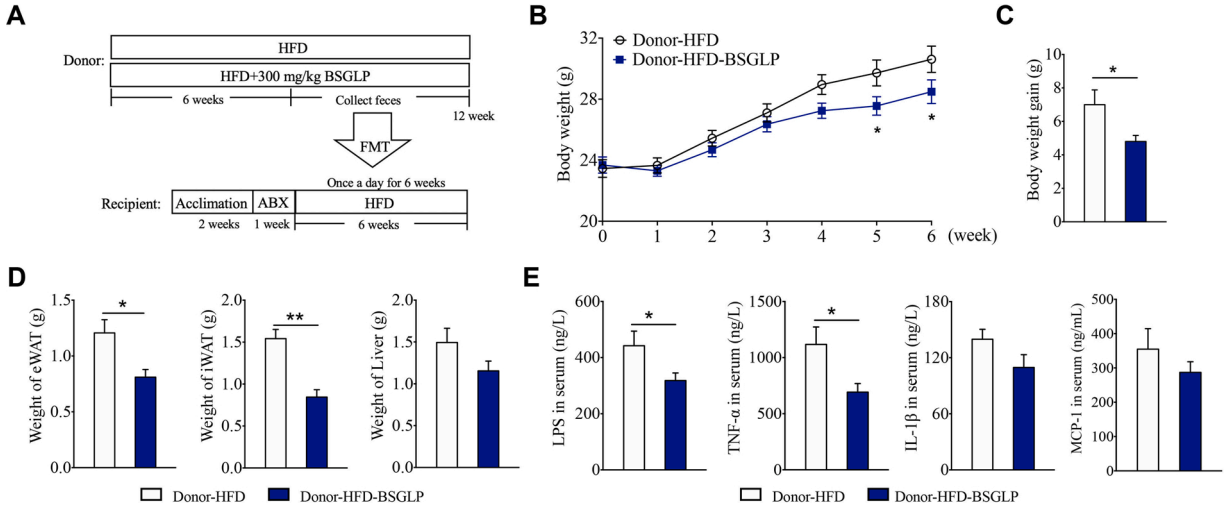

Fig. 9. FMT from HFD-300 mg/kg BSGLP-treated mice reduces obesity and inflammation in HFD-fed recipient mice. (A) Diagram illustrating the experimental scheme of FMT. Antibiotics (ABX) treated mice were transplanted with fecal microbiota from HFD-fed donors or HFD-300 mg/kg BSGLP treated mice. (B) Body weight curve. (C) Body weight gain. (D) Weight of eWAT, iWAT, and liver. (E) Serum level of LPS, TNF-α, IL-1β, and MCP-1. (n = 7 mice/group). Data are presented as means ± SEM and analyzed using student's unpaired *t*-test. $^{*}P < 0.05$, $^{**}P < 0.01$.

from the sporoderm-broken spores of *G. lucidum* has never been reported before.

In this study, we showed for the first time that BSGLP inhibited dietary-induced fat accumulation, hepatic steatosis, bodyweight increase, hyperlipidemia, and inflammation, which is associated with its improvement on HFD-induced microbiota dysbiosis, gut barrier impairment, and increased SCFAs. Our data revealed that BSGLP reduced LPS level, accompanied by the suppression of TLR4/NF-κB signaling pathway in adipose tissue (Fig. 10). Our study provides an important theoretical basis for future research on the pharmacological effects of BSGLP, which can be used as a prebiotic agent for the prevention of obesity and its related diseases.

The microbiota of the gut depends largely on dietary fibers and polysaccharides as energy sources, and in addition, dietary polysaccharides can have a major impact on gut microbial ecology and health of the host (Flint, Bayer, Rincon, Lamed, & White, 2008). At present, several mechanisms have been proposed to be responsible for the anti-obesity effects of dietary fibers and polysaccharides via regulating gut microbiota. Dietary fibers and polysaccharide can maintain gut barrier integrity via increasing the expression of tight junction proteins and reducing mucus-degrading bacteria in the gut, and thus reduce endotoxemia (Makki et al., 2018; Martel et al., 2017). They could also increase the amount of SCFAs and induce regulator T cells and thus regulate immunity and inhibit inflammation (Canfora et al., 2015; Makki et al., 2018). Besides, dietary fibers and polysaccharides can reduce the absorption of nutrients, inhibit digestive enzymes, and increase the growth of beneficial commensal bacteria in the gut (Makki et al., 2018; Martel et al., 2017). Our study suggests that BSGLP may inhibit obesity through the above mechanisms, including increase SCFAs level, improve gut barrier function, reduce endotoxemia, and increase beneficial bacterial production via regulating microbiota profile.

The human gut microbiota is dominated by two phyla, *Firmicutes* and *Bacteroidetes* which account for more than 90 % of all the bacterial species in the gut (Eckburg et al., 2005; Turnbaugh et al., 2006). Although many studies point towards a relative increase in *Firmicutes/Bacteroidetes* ratio as a characteristic of the "obese microbiome", the findings are inconsistent. In our study, 300 mg/kg of BSGLP dramatically increased the abundance of *Bacteroidetes* and *Bacteroides* at phylum and genus levels, respectively. It has been reported that members of the *Bacteroidetes* in particular are associated with human metabolic diseases (Johnson, Heaver, Walters, & Ley, 2017). The content of *Bacteroidetes* indicated a superlative ability to utilize polysaccharides (Backhed, Ley,

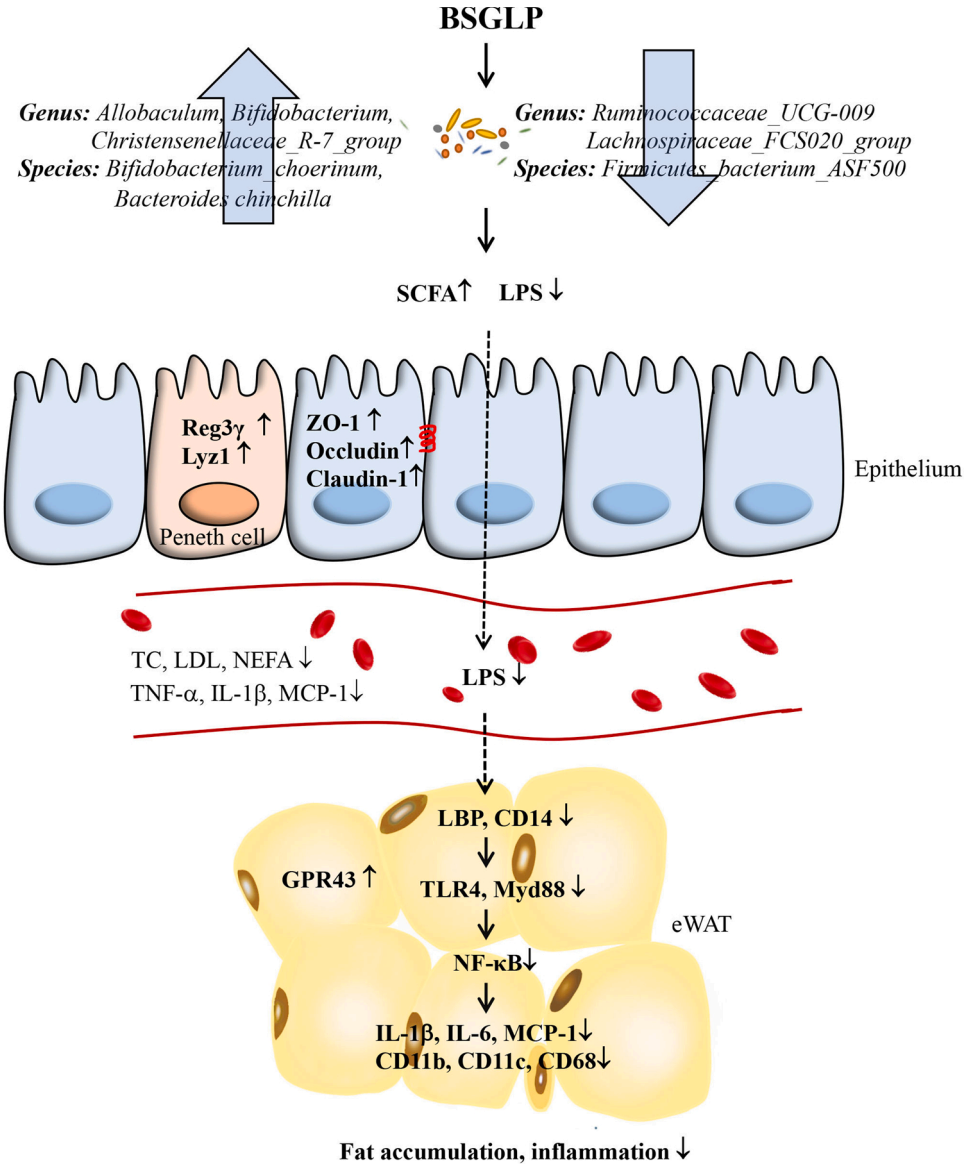

Fig. 10. Proposed mechanisms underlying the inhibitory effects of BSGLP on HFD-induced obesity and inflammation.

Sonnenburg, Peterson, & Gordon, 2005; Johnson et al., 2017). Kaoutari et al. reported that members of *Bacteroidetes* encode a proportionally high number of carbohydrate-active enzymes (CAZymes) that are key enzymes to digest polysaccharides than bacteria of other phyla (El Kaoutari, Armougom, Gordon, Raoult, & Henrissat, 2013).

We also discovered that BSGLP can increase some SCFA-producing bacteria and potential probiotics including *Allobaculum*, *Bifidobacterium,* and *Christensenellaceae_R-7_group* which have been reported negatively correlated with obesity (Liu et al., 2019; Tao et al., 2019; Wang, Tang et al., 2015; Zhang et al., 2015). Intriguingly, the probiotic *Akkermansia* which was previously reported to reduce obesity was also upregulated by BSGLP upon HFD (Everard et al., 2013). BSGLP feeding also decreased several bacterial species associated with inflammation and obesity. Reduction in beneficial bacteria, such as butyrate-producing bacteria *Bifidobacterium* has been associated with the production of systemic and adipose tissue inflammation in the host, thus causing and metabolic comorbidities such as obesity (Delzenne, Neyrinck, Backhed, & Cani, 2011; Wang, Tang et al., 2015). Chronic low-grade inflammation is one of the important characteristics of obesity-induced by HFD. Our results showed that BSGLP significantly inhibited HFD-induced inflammatory response, manifested in the reduction of inflammatory factors (TNF-α, IL-1β, and MCP-1) in serum and adipose tissue, and reduced macrophage infiltration in adipose tissue.

At the species level, BSGLP significantly increased the abundance of *Bifidobacterium_choerinum*, a probiotic in piglet against *Salmonella enterica serovar Typhimurium* infection (Splichalova et al., 2011). Consistent with our study, Wang et al. found that a combination of *Bifidobacterium* and *Salvia miltiorrhiza* polysaccharide alleviated hepatic steatosis in HFD-induced NAFLD mice (Wang et al., 2019). Interestingly, Yamin et al. reported that GLP showed prebiotic ability as it could increase the number of *Bifidobacterium* and *Lactobacillus genus* as fermented with fecal materials *in vitro* (Yamin et al., 2012). Together with these observations, our results indicate that BSGLP can improve the richness of probiotics in the gut microbiota of obese mice, and thus may serve as a prebiotic preventing the occurrence of obesity and hyperlipidemia.

Gut microbiota depends largely on plant-derived polysaccharides to be digested into SCFAs as an energy source (Flint et al., 2008). Besides, these are not only of importance in gut health and as signaling molecules, but also enter the systemic circulation and directly affect metabolism or the function of peripheral tissues, such as regulating glycogenesis and fat accumulation (Canfora et al., 2015). Among all the SCFAs, butyrate is the major intestinal fuel, supplying ~70 % of the energy needs for colonic cells, while acetate can be absorbed in the highest amount in the liver and reaches the highest peripheral concentrations than other SCFAs (Canfora et al., 2015). Concentrations of SCFAs dependent on both the production and absorption rates in the gut, which is related to dietary patterns. From our results, we found that acetate and butyrate in feces were induced upon BSGLP treatment upon HFD. Unfortunately, we were not able to test SCFAs in the serum due to lacking enough serum samples by GC–MS method. Studies have reported that the levels of serum SCFAs are consistent with the changing trend of fecal or cecal SCFAs upon dietary intervention (Dong et al., 2020; Trompette et al., 2014). Therefore, SCFAs may be important gut metabolites involved in the fermentation of BSGLP that have important anti-obesity functions in HFD-fed mice that target both the intestinal and the peripheral tissues, such as adipose tissue. GPR43, one of the key SCFAs sensing receptors, has been reported playing a crucial role in the crosstalk of the gut microbiota with host metabolism (Canfora et al., 2015). Most studies showed that GPR43 knockout is positively correlated with the occurrence of obesity, glucose intolerance, and other metabolic syndromes (Kimura et al., 2013; McNelis et al., 2015; Tolhurst et al., 2012). Overexpression of GPR43 specifically in adipose tissue remained lean even fed with HFD in mice (Kimura et al., 2013). In our study, HFD significantly decreased the expression of GPR43 in eWAT. We also observed that BSGLP significantly increased GPR43 expression under HFD in eWAT, which indicates that BSGLP inhibits HFD-induced obesity might be closely related to the activation of GPR43. Therefore, the bacterial metabolite SCFAs that modified by BSGLP was possibly absorbed into the circulatory system and further acted on the GPR43 receptor in adipose tissue, which might be the potential mechanism for the anti-obesogenic effect of BSGLP.

Gut microbiota dysbiosis increases LPS level and causes damage to the gut barrier, which eventually results in endotoxemia and systemic chronic inflammation (Zhao, 2013). The addition of probiotics can effectively alleviate the generation of intestinal endotoxin LPS and improve the gut barrier function (Wang, Tang et al., 2015). The tight junction of the intestinal epithelium is the determinant of the gut barrier, and antimicrobial peptides are the ancient components of immune defense that control host interaction with gut microbiota (Kurashima & Kiyono, 2017). LPS is recognized by its binding protein LBP to form a complex which transfers the LPS to CD14, and then activates transmembrane protein TLR4 and subsequently promotes activation of NF-κB and regulates the expression of inflammatory factors (Winer et al., 2016; Zhao, 2013). Myd88 is a key adaptor of TLR4 and plays an important role in obesity and diabetes. Its deletion in the central nervous system or intestinal epithelial cells has been shown to inhibit HFD-induced body weight gain and glucose intolerance (Everard et al., 2014; Kleinridders et al., 2009). In consistent with the above hypothesis, our results suggest that BSGLP ameliorates HFD-induced endotoxemia through maintaining gut barrier and gut immunity by increasing the expression of tight junction protein and the secretion of antimicrobial peptides and inhibiting TLR4/Myd88/NF-κB expressions in HFD-fed mice.

Although several studies reported that GLP from the fruiting body or mycelium of *G. lucidum* has the effects of reducing high blood glucose in the Type 2 diabetes model (Chang et al., 2015; Li et al., 2011; Xu et al., 2017), only very few reports showing the effect of BSGLP on blood glucose. Unfortunately, although BSGLP significantly improved hyperlipidemia that is consistent with previous reports (Li et al., 2011; Xu et al., 2017), it had no effects on glucose tolerance upon HFD in our study. A literature search revealed that, our result is consistent with a few clinical trials that *G. lucidum* showed little or no effects on blood glucose levels of diabetic patients or subjects with hypertension and high cholesterol (Chu et al., 2012; Klupp, Kiat, Bensoussan, Steiner, & Chang, 2016). The different results regarding the effects of GLP on glucose tolerance and lipid metabolism may be explained by differences in the design of the experiment, the source of GLP, and maybe the technique each investigator used. The exact role of BSGLP on glucose tolerance and insulin sensitivity should be further examined in the future.

FMT study using germ-free mice or antibiotics treated pseudo germ-free mice are necessary to elucidate the exact role of BSLGP in obesity. To investigate the beneficial effects of BSGLP-altered microbiota, we used pseudo germ-free mice and conducted FMT study. Our results showed that the pseudo germ-free mice reconstituted with the gut microbiota of BSGLP treated mice gained less body weight, fat accumulation, and serum inflammatory cytokines than pseudo germ-free mice colonized with the fecal microbiota of HFD controls. This study suggested that gut bacteria were involved in the beneficial effects of BSGLP in inhibiting HFD-induced obesity and inflammation. One of the major open questions is whether the changes in intestinal microbiota precede the development of obesity or if they are a reflection of the obese phenotype (Sanmiguel, Gupta, & Mayer, 2015). This is also one of the limitations of our study. Due to the intricate interrelationship among diet, microbiota, immunity, and obesity development, it is a difficult question to answer at present, which need to be further studied in the future.

5. Conclusion

In conclusion, our results showed that GLP extracted from

sporoderm-broken spores of *G. lucidum* significantly reduced fat accumulation, hepatic steatosis, inflammation, and hyperlipidemia in HFD-fed mice. As summarized in Fig. 10, the beneficial effects of BSGLP against obesity may be associated with its modulation of gut microbiota, gut barrier, SCFAs production, activation of GPR43, and inhibition of TLR4/Myd88/NF-κB signaling pathway. Our findings suggest that BSGLP may be used as a prebiotic agent for targeting the gut microbiota against obesity, hyperlipidemia, and inflammation-related diseases.

Availability of data and materials

The datasets used and/or analyzed during the current study would be available from the corresponding author Xingya Wang on request.

CRediT authorship contribution statement

Tingting Sang: Investigation, Data curation, Methodology, Software, Validation, Visualization, Writing - original draft, Funding acquisition. **Chengjie Guo:** Investigation, Data curation, Software, Methodology, Validation. **Dandan Guo:** Investigation, Data curation, Software. **Jianjun Wu:** Investigation, Data curation, Methodology, Software. **Yujie Wang:** Investigation, Data curation, Software. **Ying Wang:** Investigation, Data curation. **Jiajun Chen:** Investigation, Data curation. **Chaojie Chen:** Investigation, Data curation. **Kaikai Wu:** Investigation. **Kun Na:** Investigation. **Kang Li:** Investigation. **Liu Fang:** Investigation. **Cuiling Guo:** Investigation. **Xingya Wang:** Conceptualization, Investigation, Data curation, Methodology, Writing - review & editing, Visualization, Validation, Project administration, Supervision, Resources, Funding acquisition.

Declaration of Competing Interest

The authors report no declarations of interest.

Acknowledgements

This study is supported by the National Natural Science Foundation of China (NSFC), Grant Number: 81973521 (X. Wang) and 81473397 (X. Wang); Science Foundation of Zhejiang Chinese Medical University, Grant Number: KC201909 (T. Sang) and SZZ201807 (T. Sang). We wish to thank Chao Jiang and Yuehan Qi at Zhejiang Chinese Medical University animal facility for their kind help with animal care. We thank Cheng Chen at the laboratory of the pathology of Zhejiang Chinese Medical University for his technical support.

Appendix A. Supplementary data

Supplementary material related to this article can be found, in the online version, at doi:https://doi.org/10.1016/j.carbpol.2020.117594.

References

Anhe, F. F., Nachbar, R. T., Varin, T. V., Trottier, J., Dudonne, S., Le Barz, M., et al. (2018). Treatment with camu camu (Myrciaria dubia) prevents obesity by altering the gut microbiota and increasing energy expenditure in diet-induced obese mice. *Gut, 68*, 453–464.

Backhed, F., Ley, R. E., Sonnenburg, J. L., Peterson, D. A., & Gordon, J. I. (2005). Host-bacterial mutualism in the human intestine. *Science, 307*(5717), 1915–1920.

Bishop, K. S., Kao, C. H., Xu, Y., Glucina, M. P., Paterson, R. R., & Ferguson, L. R. (2015). From 2000years of Ganoderma lucidum to recent developments in nutraceuticals. *Phytochemistry, 114*, 56–65.

Bozec, A., & Hannemann, N. (2016). Mechanism of regulation of adipocyte numbers in adult organisms through differentiation and apoptosis homeostasis. *Journal of Visualized Experiments: JoVE, 112*, 53822.

Canfora, E. E., Jocken, J. W., & Blaak, E. E. (2015). Short-chain fatty acids in control of body weight and insulin sensitivity. *Nature Reviews Endocrinology, 11*(10), 577–591.

Chang, C. J., Lin, C. S., Lu, C. C., Martel, J., Ko, Y. F., Ojcius, D. M., et al. (2015). Ganoderma lucidum reduces obesity in mice by modulating the composition of the gut microbiota. *Nature Communications, 6*, 7489.

Chen, M., Xiao, D., Liu, W., Song, Y., Zou, B., Li, L., et al. (2019). Intake of Ganoderma lucidum polysaccharides reverses the disturbed gut microbiota and metabolism in type 2 diabetic rats. *International Journal of Biological Macromolecules, 155*, 890–902.

Chen, S., Li, X., Liu, L., Liu, C., & Han, X. (2018). Ophiopogonin D alleviates high-fat diet-induced metabolic syndrome and changes the structure of gut microbiota in mice. *FASEB Journal, 32*(3), 1139–1153.

Chu, T. T., Benzie, I. F., Lam, C. W., Fok, B. S., Lee, K. K., & Tomlinson, B. (2012). Study of potential cardioprotective effects of Ganoderma lucidum (Lingzhi): Results of a controlled human intervention trial. *The British Journal of Nutrition, 107*(7), 1017–1027.

Collaboration, N. C. D. R. F. (2017). Worldwide trends in body-mass index, underweight, overweight, and obesity from 1975 to 2016: A pooled analysis of 2416 population-based measurement studies in 128.9 million children, adolescents, and adults. *Lancet, 390*(10113), 2627–2642.

Delzenne, N. M., Neyrinck, A. M., Backhed, F., & Cani, P. D. (2011). Targeting gut microbiota in obesity: Effects of prebiotics and probiotics. *Nature Reviews Endocrinology, 7*(11), 639–646.

Desai, M. S., Seekatz, A. M., Koropatkin, N. M., Kamada, N., Hickey, C. A., Wolter, M., et al. (2016). A dietary fiber-deprived gut microbiota degrades the colonic mucus barrier and enhances pathogen susceptibility. *Cell, 167*(5), 1339-1353 e1321.

Dong, Y., Yan, H., Zhao, X., Lin, R., Lin, L., Ding, Y., et al. (2020). Gu-ben-Fang-Xiao decoction ameliorated murine asthma in remission stage by modulating microbiota-acetate-Tregs Axis. *Frontiers in Pharmacology, 11*, 549.

Eckburg, P. B., Bik, E. M., Bernstein, C. N., Purdom, E., Dethlefsen, L., Sargent, M., et al. (2005). Diversity of the human intestinal microbial flora. *Science, 308*(5728), 1635–1638.

Eisinger, K., Liebisch, G., Schmitz, G., Aslanidis, C., Krautbauer, S., & Buechler, C. (2014). Lipidomic analysis of serum from high fat diet induced obese mice. *International Journal of Molecular Sciences, 15*(2), 2991–3002.

El Kaoutari, A., Armougom, F., Gordon, J. I., Raoult, D., & Henrissat, B. (2013). The abundance and variety of carbohydrate-active enzymes in the human gut microbiota. *Nature Reviews Microbiology, 11*(7), 497–504.

Everard, A., Belzer, C., Geurts, L., Ouwerkerk, J. P., Druart, C., Bindels, L. B., et al. (2013). Cross-talk between Akkermansia muciniphila and intestinal epithelium controls diet-induced obesity. *Proceedings of the National Academy of Sciences of the United States of America, 110*(22), 9066–9071.

Everard, A., Geurts, L., Caesar, R., Van Hul, M., Matamoros, S., Duparc, T., et al. (2014). Intestinal epithelial MyD88 is a sensor switching host metabolism towards obesity according to nutritional status. *Nature Communications, 5*, 5648.

Flint, H. J., Bayer, E. A., Rincon, M. T., Lamed, R., & White, B. A. (2008). Polysaccharide utilization by gut bacteria: Potential for new insights from genomic analysis. *Nature Reviews Microbiology, 6*(2), 121–131.

Fu, Y., Shi, L., & Ding, K. (2019). Structure elucidation and anti-tumor activity in vivo of a polysaccharide from spores of Ganoderma lucidum (Fr.) Karst. *International Journal of Biological Macromolecules, 141*, 693–699.

Fujisaka, S., Avila-Pacheco, J., Soto, M., Kostic, A., Dreyfuss, J. M., Pan, H., et al. (2018). Diet, genetics, and the gut microbiome drive dynamic changes in plasma metabolites. *Cell Reports, 22*(11), 3072–3086.

Hayek, T., Ito, Y., Azrolan, N., Verdery, R. B., Aalto-Setala, K., Walsh, A., et al. (1993). Dietary fat increases high density lipoprotein (HDL) levels both by increasing the transport rates and decreasing the fractional catabolic rates of HDL cholesterol ester and apolipoprotein (Apo) A-I. Presentation of a new animal model and mechanistic studies in human Apo A-I transgenic and control mice. *The Journal of Clinical Investigation, 91*(4), 1665–1671.

Heymsfield, S. B., & Wadden, T. A. (2017). Mechanisms, pathophysiology, and management of obesity. *The New England Journal of Medicine, 376*(3), 254–266.

Hu, J., Liu, Y., Cheng, L., Shi, R., Qayum, A., Bilawal, A., et al. (2020). Comparison in bioactivity and characteristics of Ginkgo biloba seed polysaccharides from four extract pathways. *International Journal of Biological Macromolecules, 159*, 1156–1164.

Huo, W., Feng, Z., Hu, S., Cui, L., Qiao, T., Dai, L., et al. (2020). Effects of polysaccharides from wild morels on immune response and gut microbiota composition in non-treated and cyclophosphamide-treated mice. *Food & Function, 11*(5), 4291–4303.

Jiang, T., Gao, X., Wu, C., Tian, F., Lei, Q., Bi, J., et al. (2016). Apple-derived pectin modulates gut microbiota, improves gut barrier function, and attenuates metabolic endotoxemia in rats with diet-induced obesity. *Nutrients, 8*(3), 126.

Johnson, E. L., Heaver, S. L., Walters, W. A., & Ley, R. E. (2017). Microbiome and metabolic disease: Revisiting the bacterial phylum Bacteroidetes. *Journal of Molecular Medicine (Berlin), 95*(1), 1–8.

Khan, I., Huang, G., Li, X. A., Liao, W., Leong, W. K., Xia, W., et al. (2019). Mushroom polysaccharides and jiaogulan saponins exert cancer preventive effects by shaping the gut microbiota and microenvironment in Apc(Min/+) mice. *Pharmacological Research, 148*, Article 104448.

Kim, H., Suh, H. J., Kang, C. M., Lee, K. H., Hwang, J. H., & Yu, K. W. (2014). Immunological activity of ginseng is enhanced by solid-state culture with Ganoderma lucidum mycelium. *Journal of Medicinal Food, 17*(1), 150–160.

Kim, M. H., Kang, S. G., Park, J. H., Yanagisawa, M., & Kim, C. H. (2013). Short-chain fatty acids activate GPR41 and GPR43 on intestinal epithelial cells to promote inflammatory responses in mice. *Gastroenterology, 145*(2), 396-406 e391-310.

Kimura, I., Ozawa, K., Inoue, D., Imamura, T., Kimura, K., et al. (2013). The gut microbiota suppresses insulin-mediated fat accumulation via the short-chain fatty acid receptor GPR43. *Nature Communications, 4*, 1829.

Kleiner, D. E., Brunt, E. M., Van Natta, M., Behling, C., Contos, M. J., Cummings, O. W., et al. (2005). Design and validation of a histological scoring system for nonalcoholic fatty liver disease. *Hepatology, 41*(6), 1313–1321.

Kleinridders, A., Schenten, D., Konner, A. C., Belgardt, B. F., Mauer, J., Okamura, T., et al. (2009). MyD88 signaling in the CNS is required for development of fatty acid-induced leptin resistance and diet-induced obesity. *Cell Metabolism, 10*(4), 249–259.
Klupp, N. L., Kiat, H., Bensoussan, A., Steiner, G. Z., & Chang, D. H. (2016). A double-blind, randomised, placebo-controlled trial of Ganoderma lucidum for the treatment of cardiovascular risk factors of metabolic syndrome. *Scientific Reports, 6*, 29540.
Kurashima, Y., & Kiyono, H. (2017). Mucosal ecological network of epithelium and immune cells for gut homeostasis and tissue healing. *Annual Review of Immunology, 35*, 119–147.
Li, F., Zhang, Y., & Zhong, Z. (2011). Antihyperglycemic effect of ganoderma lucidum polysaccharides on streptozotocin-induced diabetic mice. *International Journal of Molecular Sciences, 12*(9), 6135–6145.
Li, J., Gu, F., Cai, C., Hu, M., Fan, L., Hao, J., et al. (2020). Purification, structural characterization, and immunomodulatory activity of the polysaccharides from Ganoderma lucidum. *International Journal of Biological Macromolecules, 143*, 806–813.
Liang, Z., Yuan, Z., Li, G., Fu, F., & Shan, Y. (2018). Hypolipidemic, antioxidant, and antiapoptotic effects of polysaccharides extracted from reishi mushroom, Ganoderma lucidum (Leysser: Fr) Karst, in mice fed a high-fat diet. *Journal of Medicinal Food, 21*(12), 1218–1227.
Liu, Y., Li, T., Alim, A., Ren, D., Zhao, Y., & Yang, X. (2019). Regulatory effects of Stachyose on colonic and hepatic inflammation, gut microbiota dysbiosis, and peripheral CD4(+) t cell distribution abnormality in high-fat diet-fed mice. *Journal of Agricultural and Food Chemistry, 67*(42), 11665–11674.
Liu, Y., Wang, C., Li, J., Li, T., Zhang, Y., Liang, Y., et al. (2020). Phellinus linteus polysaccharide extract improves insulin resistance by regulating gut microbiota composition. *FASEB Journal, 34*(1), 1065–1078.
Makki, K., Deehan, E. C., Walter, J., & Backhed, F. (2018). The impact of dietary fiber on gut microbiota in host health and disease. *Cell Host & Microbe, 23*(6), 705–715.
Martel, J., Ojcius, D. M., Chang, C. J., Lin, C. S., Lu, C. C., Ko, Y. F., et al. (2017). Anti-obesogenic and antidiabetic effects of plants and mushrooms. *Nature Reviews Endocrinology, 13*(3), 149–160.
Maurizi, G., Della Guardia, L., Maurizi, A., & Poloni, A. (2018). Adipocytes properties and crosstalk with immune system in obesity-related inflammation. *Journal of Cellular Physiology, 233*(1), 88–97.
McNelis, J. C., Lee, Y. S., Mayoral, R., van der Kant, R., Johnson, A. M., Wollam, J., et al. (2015). GPR43 potentiates beta-cell function in obesity. *Diabetes, 64*(9), 3203–3217.
Pan, H., Wang, Y., Na, K., Wang, Y., Wang, L., Li, Z., et al. (2019). Autophagic flux disruption contributes to Ganoderma lucidum polysaccharide-induced apoptosis in human colorectal cancer cells via MAPK/ERK activation. *Cell Death & Disease, 10*(6), 456.
Sanmiguel, C., Gupta, A., & Mayer, E. A. (2015). Gut microbiome and obesity: A plausible explanation for obesity. *Current Obesity Reports, 4*(2), 250–261.
Sommer, F., & Backhed, F. (2013). The gut microbiota–masters of host development and physiology. *Nature Reviews Microbiology, 11*(4), 227–238.
Sonnenburg, J. L., & Backhed, F. (2016). Diet-microbiota interactions as moderators of human metabolism. *Nature, 535*(7610), 56–64.
Splichalova, A., Trebichavsky, I., Rada, V., Vlkova, E., Sonnenborn, U., & Splichal, I. (2011). Interference of Bifidobacterium choerinum or Escherichia coli Nissle 1917 with Salmonella Typhimurium in gnotobiotic piglets correlates with cytokine patterns in blood and intestine. *Clinical and Experimental Immunology, 163*(2), 242–249.
Stevens, B. R., Goel, R., Seungbum, K., Richards, E. M., Holbert, R. C., Pepine, C. J., et al. (2018). Increased human intestinal barrier permeability plasma biomarkers zonulin and FABP2 correlated with plasma LPS and altered gut microbiome in anxiety or depression. *Gut, 67*(8), 1555–1557.
Sun, X., Wang, H., Han, X., Chen, S., Zhu, S., & Dai, J. (2014). Fingerprint analysis of polysaccharides from different Ganoderma by HPLC combined with chemometrics methods. *Carbohydrate Polymers, 114*, 432–439.
Tao, S., Bai, Y., Zhou, X., Zhao, J., Yang, H., Zhang, S., et al. (2019). In vitro fermentation characteristics for different ratios of soluble to insoluble dietary fiber by fresh fecal microbiota from growing pigs. *ACS Omega, 4*(12), 15158–15167.
Tilg, H., Zmora, N., Adolph, T. E., & Elinav, E. (2019). The intestinal microbiota fuelling metabolic inflammation. *Nature Reviews Immunology, 20*(1), 40–54.
Tolhurst, G., Heffron, H., Lam, Y. S., Parker, H. E., Habib, A. M., Diakogiannaki, E., et al. (2012). Short-chain fatty acids stimulate glucagon-like peptide-1 secretion via the G-protein-coupled receptor FFAR2. *Diabetes, 61*(2), 364–371.
Trompette, A., Gollwitzer, E. S., Yadava, K., Sichelstiel, A. K., Sprenger, N., Ngom-Bru, C., et al. (2014). Gut microbiota metabolism of dietary fiber influences allergic airway disease and hematopoiesis. *Nature Medicine, 20*(2), 159–166.
Turnbaugh, P. J., Hamady, M., Yatsunenko, T., Cantarel, B. L., Duncan, A., Ley, R. E., et al. (2009). A core gut microbiome in obese and lean twins. *Nature, 457*(7228), 480–484.
Turnbaugh, P. J., Ley, R. E., Mahowald, M. A., Magrini, V., Mardis, E. R., & Gordon, J. I. (2006). An obesity-associated gut microbiome with increased capacity for energy harvest. *Nature, 444*(7122), 1027–1031.
Ussar, S., Griffin, N. W., Bezy, O., Fujisaka, S., Vienberg, S., Softic, S., et al. (2015). Interactions between gut microbiota, host genetics and diet modulate the predisposition to obesity and metabolic syndrome. *Cell Metabolism, 22*(3), 516–530.
Wang, W., Xu, A. L., Li, Z. C., Li, Y., Xu, S. F., Sang, H. C., et al. (2019). Combination of probiotics and Salvia miltiorrhiza polysaccharide alleviates hepatic steatosis via gut microbiota modulation and insulin resistance improvement in high fat-induced NAFLD mice. *Diabetes & Metabolism Journal, 44*(2), 336–348.
Wang, Y., Liu, Y., Yu, H., Zhou, S., Zhang, Z., Wu, D., et al. (2017). Structural characterization and immuno-enhancing activity of a highly branched water-soluble beta-glucan from the spores of Ganoderma lucidum. *Carbohydrate Polymers, 167*, 337–344.
Wang, J. H., Bose, S., Kim, H. G., Han, K. S., & Kim, H. (2015). Fermented Rhizoma Atractylodis Macrocephalae alleviates high fat diet-induced obesity in association with regulation of intestinal permeability and microbiota in rats. *Scientific Reports, 5*, 8391.
Wang, J., Tang, H., Zhang, C., Zhao, Y., Derrien, M., Rocher, E., et al. (2015). Modulation of gut microbiota during probiotic-mediated attenuation of metabolic syndrome in high fat diet-fed mice. *The ISME Journal, 9*(1), 1–15.
Winer, D. A., Luck, H., Tsai, S., & Winer, S. (2016). The intestinal immune system in obesity and insulin resistance. *Cell Metabolism, 23*(3), 413–426.
Wu, J., Chen, M., Shi, S., Wang, H., Li, N., Su, J., et al. (2017). Hypoglycemic effect and mechanism of a pectic polysaccharide with hexenuronic acid from the fruits of Ficus pumila L. in C57BL/KsJ db/db mice. *Carbohydrate Polymers, 178*, 209–220.
Wu, T. R., Lin, C. S., Chang, C. J., Lin, T. L., Martel, J., Ko, Y. F., et al. (2019). Gut commensal Parabacteroides goldsteinii plays a predominant role in the anti-obesity effects of polysaccharides isolated from Hirsutella sinensis. *Gut, 68*(2), 248–262.
Xu, S., Dou, Y., Ye, B., Wu, Q., Wang, Y., Hu, M., et al. (2017). Ganoderma lucidum polysaccharides improve insulin sensitivity by regulating inflammatory cytokines and gut microbiota composition in mice. *Journal of Functional Foods, 38*, 545–552.
Xu, Y., Zhang, X., Yan, X. H., Zhang, J. L., Wang, L. Y., Xue, H., et al. (2019). Characterization, hypolipidemic and antioxidant activities of degraded polysaccharides from Ganoderma lucidum. *International Journal of Biological Macromolecules, 135*, 706–716.
Yamin, S., Shuhaimi, M., Arbakariya, A., Fatimah, A. B., Khalilah, A. K., Anas, O., et al. (2012). Effect of Ganoderma lucidum polysaccharides on the growth of Bifidobacterium spp. as assessed using real-time PCR. *International Food Research Journal, 19*(3), 1199–1205.
Ye, L., Zhang, J., Zhou, K., Yang, Y., Zhou, S., Jia, W., et al. (2008). Purification, NMR study and immunostimulating property of a fucogalactan from the fruiting bodies of Ganoderma lucidum. *Planta Medica, 74*(14), 1730–1734.
Zhang, J., Liu, Y., Tang, Q., Zhou, S., Feng, J., & Chen, H. (2019). Polysaccharide of Ganoderma and its bioactivities. *Advances in Experimental Medicine and Biology, 1181*, 107–134.
Zhang, X., Zhao, Y., Xu, J., Xue, Z., Zhang, M., Pang, X., et al. (2015). Modulation of gut microbiota by berberine and metformin during the treatment of high-fat diet-induced obesity in rats. *Scientific Reports, 5*, 14405.
Zhao, L. (2013). The gut microbiota and obesity: From correlation to causality. *Nature Reviews Microbiology, 11*(9), 639–647.